Comprehensive Assessment and Mathematical Modeling of T Cell Population Dynamics and Homeostasis[1]

Véronique Thomas-Vaslin,[2,3]*† Hester Korthals Altes,[3,4]‡ Rob J. de Boer,[5]§ and David Klatzmann[5]*†

Our current view of T cell differentiation and population dynamics is assembled from pieces of data obtained from separate experimental systems and is thus patchy. We reassessed homeostasis and dynamics of T cells 1) by generating a mathematical model describing the spatiotemporal features of T cell differentiation, and 2) by fitting this model to experimental data generated by disturbing T cell differentiation through transient depletion of dividing T cells in mice. This specific depletion was obtained by administration of ganciclovir to mice expressing the conditional thymidine kinase suicide gene in T cells. With this experimental approach, we could derive quantitative parameters describing the cell fluxes, residence times, and rates of import, export, proliferation, and death across cell compartments for thymocytes and recent thymic emigrants (RTEs). Among other parameters, we show that 93% of thymocytes produced before single-positive stages are eliminated through the selection process. Then, a post-selection peripheral expansion of naive T cells contributes three times more to naive T cell production than the thymus, with half of the naive T cells consisting of dividing RTEs. Altogether, this work provides a quantitative population dynamical framework of thymocyte development, RTEs, and naive T cells. ***The Journal of Immunology,*** **2008, 180: 2240–2250.**

The high turnover, migration, and recirculation of lymphoid cell populations are key features of a resilient immune system regulated by homeostasis (1). The immune system efficacy is guaranteed both by the diverse repertoire of the naive cells (2) and by the rapid memory response of previously selected and expanded Ag-experienced T cells (3). Because immune responses are associated with major expansions of specific T cells followed by T cell death, homeostatic regulation is essential to maintain the equilibrium between cell production and cell death, and between naive and effector/memory T cells, as well as to preserve repertoire diversity.

Elements of the dynamics of peripheral T lymphocyte populations and their precursors in the thymus have been studied using various experimental approaches in rodents. These studies were based on cellular DNA labeling (4–8), targeted expression of MHC molecules (9, 10), or the tracking of migration of labeled recent thymic emigrants (RTE)[6] (11–13). They also involved the artificial increase (14) or decrease (15) of thymic output, transfer of isolated cell populations (16, 17), or in vitro systems of T cell development (18). Collectively, these studies have provided estimates for proliferation rates, cell lifespans, daily export, or cell death and renewal rates in various cellular compartments. Different mechanisms for homeostasis were proposed (19–21). However, these data gathered with various experimental methods are difficult to combine into a single model accounting for the quantitative aspects of cell dynamics. In addition, the temporal parameters of the population dynamics of T cells in response to a short lymphopenia have only partially been established (22–26). This leaves us with a puzzling, complex, and incomplete view of thymocyte and peripheral T cell dynamics.

In the present study, we used a single experimental system of transient perturbation of T lymphocyte homeostasis, in combination with a mathematical model, to quantify the T cell differentiation dynamics in mice. We induced a temporary cell depletion of the immature TCR^- $CD4^-CD8^-$ thymocytes through to the mature peripheral CD4 and CD8 T cells in young adult mice with a wild-type T cell repertoire. This was achieved using mice transgenic for the conditional *HSV1-TK* (*TK*) suicide gene (27–29). Expression of the *TK* gene allows eukaryotic cells to metabolize ganciclovir (GCV) into a triphosphate active form, which can be incorporated in the DNA of dividing cells, blocking DNA elongation and inducing cell death. Cell killing in our system is thus strictly conditioned by three simultaneous constraints: *TK* expression, GCV administration, and cell division. In fact, our experimental system corresponds to "soft" thymectomy (Tx), as this procedure temporarily blocks thymic output without the side effects associated with surgery.

*Université Pierre et Marie Curie-Paris 06, Unité Mixte de Recherche 7087, Biologie et Thérapeutique des Pathologies Immunitaires, Paris, France; †Centre National de la Recherche Scientifique, Unité Mixte de Recherche 7087, Biologie et Thérapeutique des Pathologies Immunitaires, Paris, France; ‡Population Biology, Institute for Biodiversity and Ecosystem Dynamics, University of Amsterdam, Amsterdam, The Netherlands; and §Theoretical Biology and Bioinformatics, Utrecht University, Utrecht, The Netherlands

Received for publication July 24, 2007. Accepted for publication December 4, 2007.

The costs of publication of this article were defrayed in part by the payment of page charges. This article must therefore be hereby marked *advertisement* in accordance with 18 U.S.C. Section 1734 solely to indicate this fact.

[1] This work was supported by grants from Agence Nationale de la Recherche sur le SIDA, Centre National de la Recherche Scientifique, Paris 6 University, Action Thématique Concertée Vieillissement Institut National de la Santé et de la Recherche Médicale, Netherlands Organisation for Scientific Research, and CompuVac.

[2] Address correspondence and reprint requests to Dr. Véronique Thomas-Vaslin, Unité Mixte de Recherche 7087, Université Pierre et Marie Curie, Centre National de la Recherche Scientifique, CERVI Groupe Hospitalo-Universitaire Pitié-Salpêtrière, 83 Boulevard de l'Hôpital 75013 Paris, France. E-mail address: thomas@chups.jussieu.fr

[3] V.T.-V. and H.K.A. contributed equally.

[4] Current address: Centre for Infectious Disease Epidemiology, National Institute for Public Health and the Environment, Antonie van Leeuwenhoeklaan 9, 3721 MA Bilthoven, The Netherlands.

[5] R.J.d.B. and D.K. contributed equally.

[6] Abbreviations used in this paper: RTE, recent thymic emigrant; GCV, ganciclovir; DN, $CD4^-CD8^-$ double negative; Ct, cycle threshold; LN, lymph node; DP, $CD4^+CD8^+$ double positive; SP, single positive; TK, HSV-1 thymidine kinase; Tx, thymectomy; 7AAD, 7-aminoactinomycin D.

We monitored cell numbers in the different T cell compartments, from $CD4^-CD8^-$ double negative (DN) thymocytes to mature T splenocytes, at different time points during and after GCV treatment. Given the complexity of the cell dynamics in the various compartments, we developed a mathematical model based on a "conveyor-belt" type of differentiation (30). We fitted this model to our experimental results, allowing us to quantify the dynamics of thymocyte and peripheral T cell populations. Our system thus provides a more comprehensive view of T cell differentiation and population dynamics in mice at steady state, from DN thymocytes to naive T cells in the spleen. Moreover, our model improves our understanding of T cell homeostasis following transient lymphopenia.

Materials and Methods

HSV1-TK-transgenic mice

The previously described *EpCD4 HSV1-TK*-transgenic L40 mice (FVB background) (28, 31) were bred in our colonies (Nouvelle Animalerie Commune, Centre d'Exploration Fonctionnelle Pitié-Salpêtrière) under specific pathogen-free conditions. Littermates were used as TK^- mice. Mice were manipulated according to European Council Directive 86/609/EEC and with the approval of the ethic committee.

In contrast with the first TK^+-transgenic mice (23), here the *TK* transgene is under control of the EPCD4 regulatory sequences (32). TK mRNA expression was assessed by RT-PCR in highly FACS purified (>99% purity) thymic or peripheral cell populations. Total RNA was extracted using RNable (Eurobio) and cDNA was synthesized from 2 μg of each RNA sample using SuperScript II RNase H reverse transcriptase and oligo dT as primer (Invitrogen Life Technologies); 100 ng was used in each quantitative real-time PCR. The same amount of RNA and cDNA was used for each sample. Primer sequences for TK were 5′-CGAGCCGATGACT TACTGGC (forward) and 5′-CCCCGGCCGATATCTCAC (reverse) and the probe sequence was 5′-FAM-TACACCACACAACACCGCCTC GACC-TAMRA-3′ (Applied Biosystems). Primers and probe for 18S were purchased as reagent kits from Applied Biosystems. The real-time PCR was performed on an ABI Prism 7700 using TaqMan Universal PCR master mix (Applied Biosystems) in triplicates. The average threshold cycles (Ct) of the triplicates were used to calculate the fold change between lymph nodes (LN) TK^+CD4^+ and others samples. Ct for 18S was used to normalize the samples. Relative quantification was calculated using the comparative Ct method (Applied Biosystems).

The relative mRNA TK expression is of 1.43 in immature $CD3^-$DN thymocytes, 6.31 in $CD3^-$ $CD4^+CD8^+$ double-positive (DP) thymocytes and, respectively, 1 and 0.67 in CD4 and CD8 LN peripheral T cells from TK^+ mice; the background value in TK^- CD4 and CD8 LN T cells from TK^- was 0. This HSV1-TK mRNA expression from immature thymocyte stages to mature peripheral T cells is in accordance with the observed cell depletion due to the TK enzymatic activity upon GCV treatment. This contrasts with the expression of the human CD4 reporter gene under the control of EPCD4 regulatory sequences, detected only in mature CD4 and CD8 T cells, but not immature DN or DP (32).

Thymectomy

Mice were thymectomized at 6 wk of age under ketamine (150 mg/kg)/xylazine (10 mg/kg) anesthesia after a preanesthesia with robinul (1.5 μg s.c.) and dopram (Vétoquinol Lure France) (0.5 mg i.p.). Under a stereomicroscope, the upper part of the thorax was opened, and a small opening made in the pleura. The two thymic lobes were carefully removed with forceps, and the skin was closed with a silk suture. A 4- to 5-wk recovery period was observed before GCV treatment.

GCV treatment and cell preparation

To deliver GCV continuously and avoid chronic stress by repeated mouse manipulation—which can induce thymic atrophy and severely affect T cell homeostasis (33), an osmotic pump was implanted in *TK* mice on day 0, by s.c. incision under ketamine/xylazine anesthesia. GCV (Roche) was administered at a dose of 50 mg/kg/day, for 7 or 14 days by Alzet 2001 and 2002 osmotic pumps, respectively (Charles River Laboratories). Treatment was initiated between 11 and 20 wk of age; the mice were then sacrificed at various times and spleen and thymus recovered. Cell suspensions were made by mechanical dissociation, washed in PBS 3% calf serum, and living mononucleated cells were counted by trypan blue exclusion.

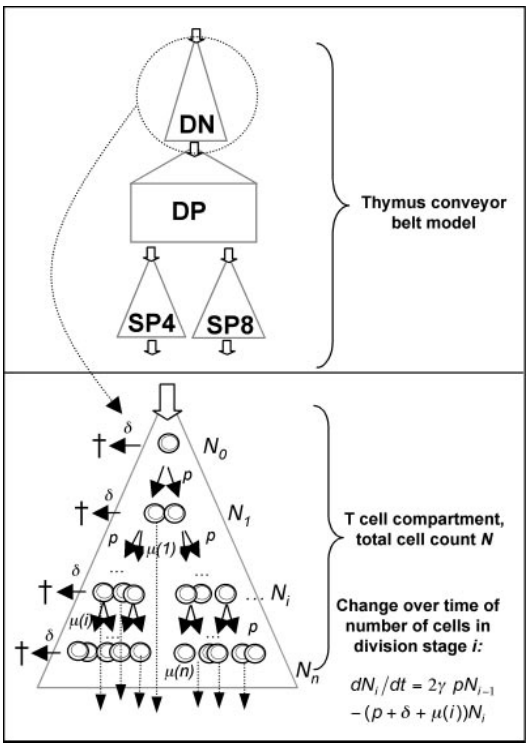

FIGURE 1. Modeling the cellular dynamics of T cell compartments in thymus and spleen. We described mathematically the dynamics of a T cell compartment (for ex. DN thymocytes), by writing a differential equation for the number of cells N_i at each division stage *i*. The generic form of this equation is given above, capturing the following processes: cells are contributed to division stage *i* from the preceding stage ($i - 1$) by division, at rate $2\gamma\, pN_{i-1}$. p is the probability that a cell divides per unit time, yielding two daughter cells, and γ is a binary "switch" that turns division "on" ($\gamma = 1$) or "off" ($\gamma = 0$). In normal circumstances, this switch is set to 1. It allows to reproduce the effect of addition of GCV: in presence of GCV, dividing cells will die rather than go into the next division stage, so no cells are contributed by division ($\gamma = 0$). Cells disappear from division stage *i* because they die at rate δN_i per unit time, or they divide at rate pN_i (going into the next division stage $i + 1$), or they differentiate into the next T cell compartment at rate $\mu(i)N_i$. The probability $\mu(i)$ of differentiating increases as cells go through more division stages: it is defined as a function of the division stage, $\mu(i) = (\alpha.i)^n$.

Immunostaining and flow cytometry

Cell surface staining was performed as previously described (28) by incubation of cell suspensions with directly labeled mAbs after blocking of FcR. Quadruple staining was done with specific anti-CD4, CD8, CD45RB, CD44, or TCR$\alpha\beta$, purchased from BD Pharmingen (BD Biosciences). Labeled cells were analyzed on a FACSCalibur (BD Biosciences). Lymphocyte cell counts were calculated as the proportion of lymphocytes, as determined by forward scatter/side scatter among the numbers of mononucleated cells per organ.

Cell cycle analysis

Quantification of cell DNA content was done by flow cytometry. Thymic or splenic cell suspensions were stained with fluorescent-labeled Abs. Cells populations were sorted on ARIA (BD Biosciences), fixed in 70% ethanol for 2 h, incubated with 7-aminoactinomycin D (7AAD; 15 μg/ml; Sigma-Aldrich) in presence of RNase (100 μg/ml) for 1 h at 37°C. Cell cycle analysis was performed on LSR2 (BD Biosciences) with 488 and 633 laser wave excitation. Dead cells and doublets were gated out and percentages of cells in S plus G_2/M phases were estimated on the basis of 7AAD expression against forward scatter.

Depletion rates under GCV therapy

The exponential depletion rate d for each cell population was obtained by fitting an exponential decay curve ($N(t) = N_0e^{-dt}$, where d corresponds to the probability that a cell dies under GCV), to the data obtained under

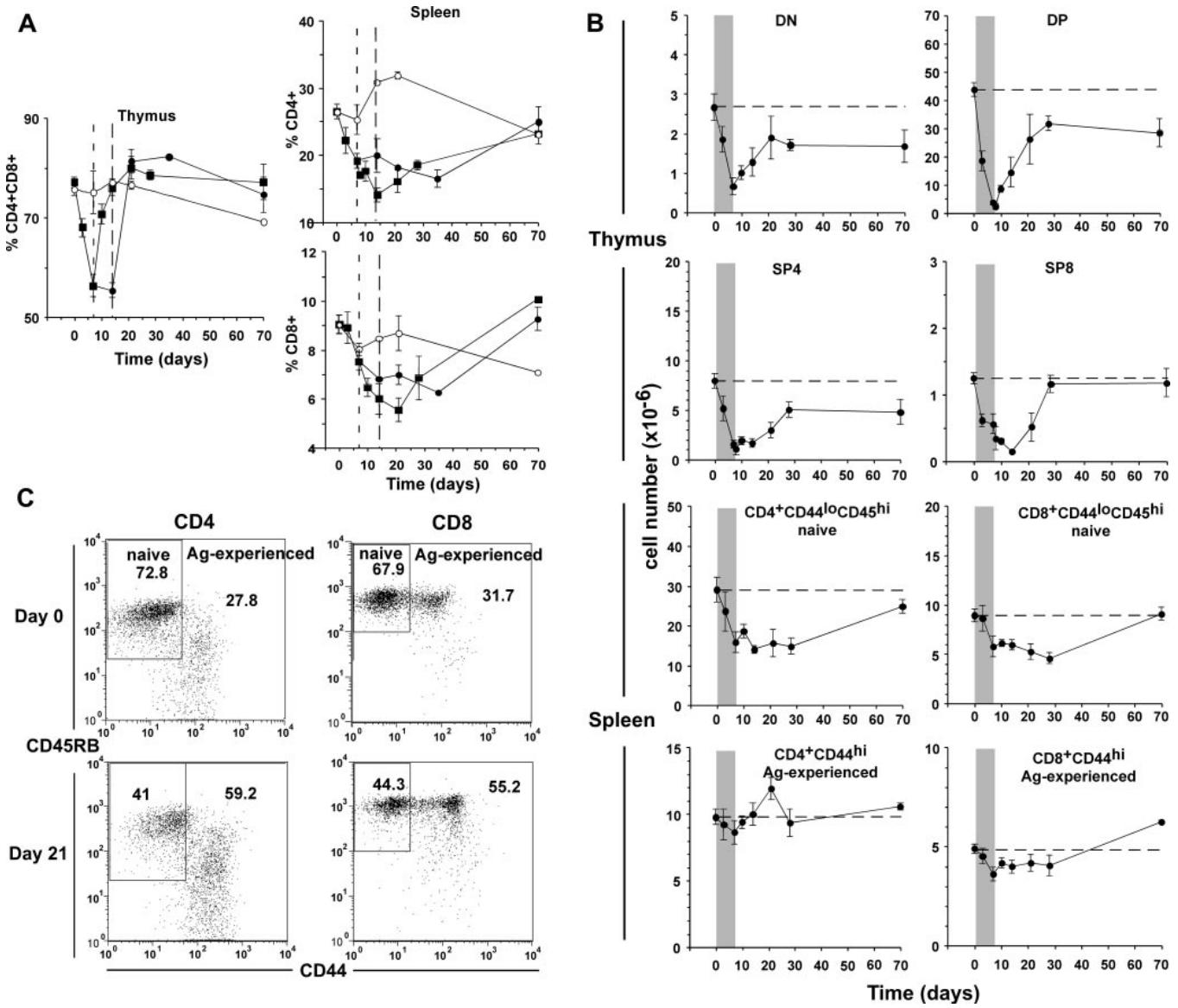

FIGURE 2. Kinetics of thymocytes and splenic T cells upon transient depletion of dividing cells. *A*, Effect of GCV on percentages of $CD4^+CD8^+$ cells in thymus and $CD4^+$ and $CD8^+$ T cells in splenic lymphocytes, as determined by flow cytometry, with a 7- (squares) or 14-day (circles) GCV treatment in TK^+ (closed symbols) or TK^- littermates (open symbols). The dashed line represents the end of the 7- or 14-day GCV treatment. *B*, TK^+ mice treated with GCV for 7 days. Mean number of $CD4^-CD8^-$ (DN) $CD4^+CD8^+$ (DP) $CD4^+CD8^-$ (SP4), $CD4^-CD8^+$ (SP8) in the thymus, and $CD44^{low}$ naive and $CD44^{high}$ Ag-experienced cells in the spleen, with SEM (individual mice depicted in Fig. 4). The shaded area is the period of GCV-treatment. The dashed line represents day 0 values. *C*, FACS dot plots of $CD4^+$- and $CD8^+$-gated splenic populations after 7-day GCV treatment in TK^+ mice: decrease in percentage naive cells ($CD45RB^{high}CD44^{low}$) between days 0 and 21, and increase in percentage Ag-experienced T cells ($CD44^{high}$).

7-day GCV treatment. To compare the depletion rates between two cell populations, we computed within each mouse the difference between cell numbers of the two populations. We then tested whether the depletion rates were different, by drawing a regression line through this difference. If the slope of the regression was significantly different from zero (*t* test on slope of the regression), the depletion rates were considered significantly different. We applied a Bonferroni correction for multiple comparisons.

Mathematical model of T cell differentiation, from early thymocytes to naive splenocytes (see supplemental material: mathematical model and formulas, section 1 and 2)[7]

We formulated a mathematical model having maximally 18 parameters to describe the differentiation from DN thymocytes to $CD44^{low}CD45RB^{high}$ naive cells as a linear DN→DP→SP→RTE→naive T splenocyte conveyor belt lacking density dependence. The dynamics were described with differential equations for the number of cells at each division stage within each T cell compartment. Fig. 1 illustrates the generic form of the model equations. For full mathematical details on the model, see the supplemental material, section 2.

The model can verbally be described as follows. Thymic precursors enter the DN cell compartment, and complete a number of divisions determined by an exit function that increases with the number of divisions. During the last division, DN cells acquire the DP phenotype. We modeled the expansion of early DP cells as a series of divisions—again dictated by an exit function—during which cells have an increasing rate of differentiation to the last stage DP. Thus, as DP cells divide, they have an increasing probability of maturing to the last stage DP where they undergo negative or positive selection before becoming single positive (SP). In the last stage, DP do not divide, and are subject to selection. There is a dramatic loss of cells between the last stage DP and early SP stage (70% of thymocytes are last stage DP cells, while 12% of thymocytes are SP cells (30)), Thus, only a fraction of last stage DP cells differentiate into SP due to the selection process. Then, SP cells complete a certain number of divisions, with late SP similarly having a greater probability than early SP of exiting the thymus. Finally, we assumed that RTE complete a number of

[7] The online version of this article contains supplemental material.

Table I. *Depletion rates and nadir under 7-day GCV treatment in TK$^+$ mice*

	N_0[a] (Million Cells)	N_{nadir}[a] (Million Cells)	t_{nadir}[b] (Days)	d[c] (/Day) (95% CI)	p[d] (Slope Regression Different from 0)
DN TCR$^-$[e]	1.6	0.4	7	0.21 (0.15–0.28)	<0.001
DP	43.8	2.4	8	0.37 (0.32–0.42)	<0.001
SP4	7.9	1.1	8	0.24 (0.18–0.31)	<0.001
SP8	1.2	0.1	14	0.14 (0.09–0.19)	<0.001
Naive CD4	29.0	14.0 (14.8)	14 (28)	0.09 (0.02–0.16)	0.01
Naive CD8	8.9	4.6	28	0.07 (0.02–0.12)	0.01
Ag-experienced CD4	9.8	8.6 (9.6)	7 (28)	0.02 (−0.02–0.06)	0.26
Ag-experienced CD8	4.9	3.6 (4.0)	7 (28)	0.05 (0.02–0.07)	<0.01

[a] Average cell number at day 0 (N_0) or at nadir (N_{nadir}) (mean and SEM are in Fig. 2*B*, individual mice in Fig. 4).
[b] Time when cells reach lowest numbers; numbers in parentheses correspond to the second nadir.
[c] Exponential depletion rates of cell populations, using data from days 0, 3, and 7.
[d] Value of p for the t test on the significance of the slope of the regression: if $p < 0.05$, the cell population is significantly depleted.
[e] DN TCR$^-$ were estimated at 60% of total DN.

divisions, during which they have an increasing probability of exiting the compartment: they may then settle in the long-lived naive cell pool, die, or possibly migrate to other lymphoid organs. To model the naive cell dynamics, we imposed a condition on the parameters, namely that 42% of cells exported from the thymus go to the spleen (11) (see supplemental material, section 3). This value was incorporated in a mathematical formula yielding the parameter f_8. We also assumed that initially, each cell population has a constant size, i.e., is at steady state.

The model was fitted to our in vivo experimental data, testing five different scenarios, each making different assumptions on the proliferation and death rates (see supplemental material, section 7). The best fit was selected according to the lowest mean squares criterion.

Mathematical simulation of Tx

Starting values for our Tx simulations were the number of RTE in each division stage estimated with our model (scenario 5) plus the number of long-lived naive cells. The decay process is described with the differential equations for $R4_i$ and $R8_i$, with division cycle i ranging from 0 to 2, and the input from the thymus being set to 0 at the moment of Tx.

Results

Kinetics of thymocytes and mature peripheral T cells, during and after 7-day depletion of dividing T cells

In our TK$^+$-transgenic mice, *TK* mRNA is expressed in thymocytes and mature peripheral T cells. In accordance with this *TK* expression pattern, GCV treatment resulted in transient depletion of thymocytes and T splenocytes in TK$^+$, but not in TK$^-$ mice (Fig. 2*A*). In the thymus of TK$^+$ mice, the percentage of CD4$^+$ CD8$^+$ (DP) cells decreased from 75 to 55%, and the nadir—the time point when a given cell population reaches its lowest size—was reached on day 7 of GCV treatment. Prolongation of treatment to 14 days did not result in further depletion but prolonged it. Whatever the treatment length, the recovery of DP cells started immediately after stopping GCV treatment. This indicates that GCV, with an intracellular half-life of 20 h (34), had no long-lasting effect on thymocytes and T cells.

In the spleen of TK$^+$ mice, the percentage of CD4$^+$ T cells dropped from 27 to 12% after a 7-day GCV treatment, with a nadir on day 14 (Fig. 2*A*). The continued decrease of T cell numbers between days 7 and 14, in the absence of GCV, likely reflects the time required for thymocyte differentiation and migration to the spleen. The nadir after a 14-day GCV treatment is less distinct, suggesting the involvement of more complex processes such as cell tissue redistribution or lymphopenia-induced proliferation. Whatever the treatment length, T cell percentages were back to almost normal levels by day 70 in all organs.

To avoid additional perturbations induced by prolonged T cell depletion, we focused our analyses on TK$^+$ mice treated with GCV for 7 days. We determined the absolute cell numbers in the

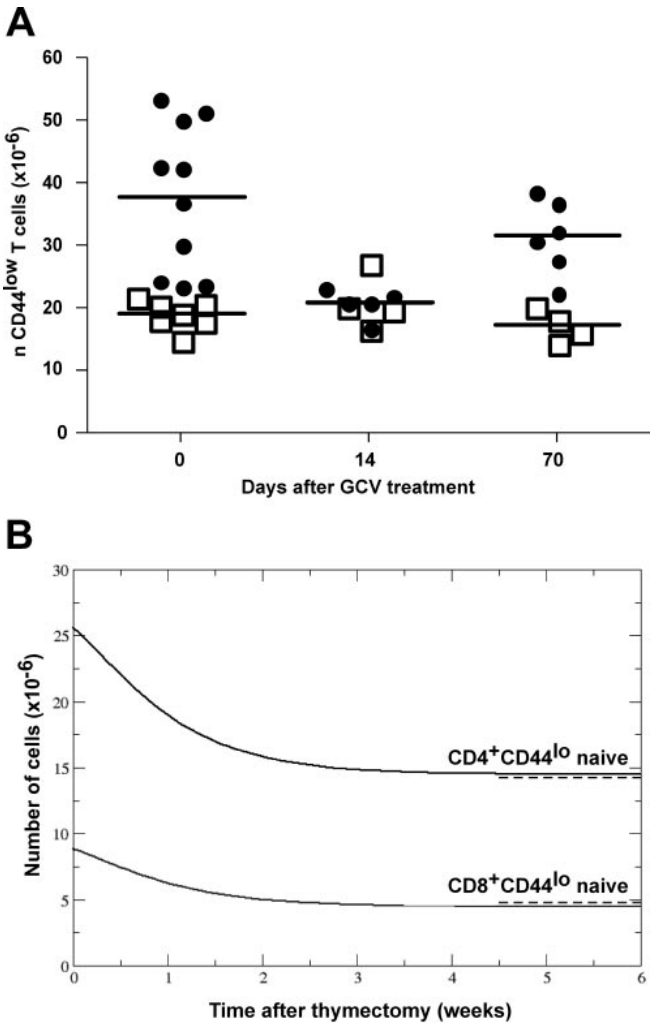

FIGURE 3. T cell dynamics in Tx mice. *A*, Total numbers CD44^{low} CD45RB^{high} (naive) T cells (CD4$^+$ and CD8$^+$) (as determined by flow cytometry) recovered in the spleen of individual euthymic (●) or Tx mice (□) mice, on days 0, 14, and 70 after 14 days of GCV treatment. Day 0 corresponds to weeks 4–5 after Tx. *B*, Simulation of Tx in mice (input from the thymus set to zero) based on parameter estimates from the model fit showing the loss of RTE in CD4 and CD8 splenocytes (continuous line). The starting values (day 0, before "Tx") are the steady state numbers of total naive CD44^{low} CD4$^+$ and CD8$^+$ T cells in the spleen (sum of RTE and long-lived naive, estimated in Table III). The dashed line represents the average number of naive CD44^{low} lymphocytes in the spleen, experimentally measured in mice 4–5 wk after a Tx.

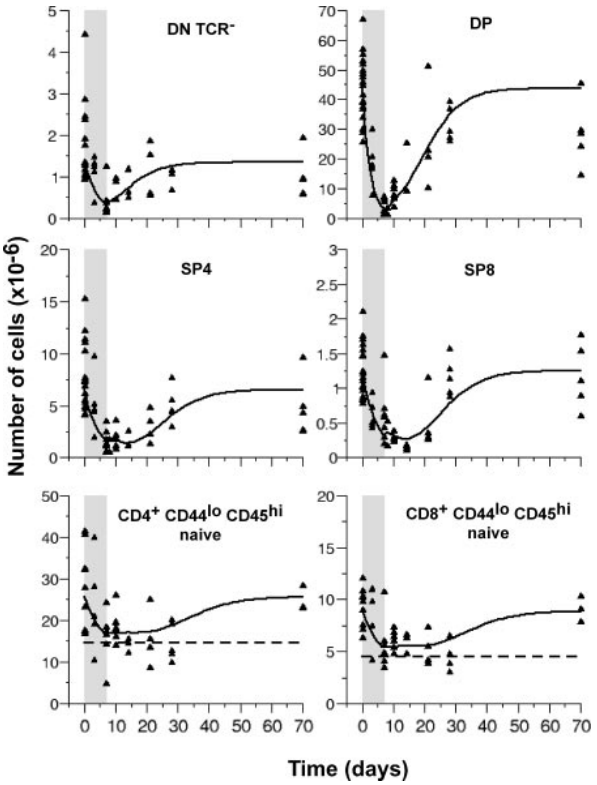

FIGURE 4. Mathematical fit of T cell kinetics upon transient depletion of dividing cells. Experimental data of Fig. 2*B* as individual points for thymic and naive splenic cells with the best-fit (continuous line) model described in the supplemental data, scenario 5. The dashed line in the $CD44^{low}CD45RB^{high}$ cells represents the long-lived naive T cell compartment in the spleen. The shaded area corresponds to the 7-day period of GCV treatment. The numbers of DN TCR^- are shown, estimated at 60% of total DN represented on Fig. 2*B* (Table I).

main thymocyte subpopulations and in mature T splenocytes at various time points during and after GCV treatment (Fig. 2*B*). In the thymus, the depletion of dividing cells induced a rapid shrinkage of the DN, DP, SP $CD4^+CD8^-$ (SP4) and $CD4^-CD8^+$ (SP8) populations, the total thymocyte count falling by ~88% in 7 days (from 56 to 6.5 million).

In the spleen, we analyzed separately the phenotypically defined $CD45RB^{high}CD44^{low}$"naive" and $CD44^{high}$"Ag-experienced" T cells (Fig. 2*C*). We observed a strong depletion of both $CD4^+$ and $CD8^+$ naive T cells, which at steady state ("day 0" in Fig. 2*C*) represent the major splenic T cell population (around 70%) in young adult mice. In contrast, there was only a modest depletion of Ag-experienced T cells during GCV treatment (Fig. 2*B*), and an increase in their percentage as the naive cell pool shrinks (Fig. 2*C*).

Estimation of depletion rates

A simple approach to analyze T cell dynamics during the depletion phase is to estimate the cell depletion rate during GCV treatment in the various thymocyte and splenocyte subpopulations using a model of exponential decay (Table I). The rate of depletion under GCV reflects 1) death of dividing cells resulting from GCV treatment, 2) "natural" cell death, and 3) decreased import from the previous cell compartment. Because the depletion rate was estimated over a short period of time (7 days), we assumed that it reflects the physiological behavior of T cells and their precursors before compensatory mechanisms may have started to counter cell loss. In the thymus, the DP cells have the highest turnover (a depletion rate of 37% per day, Table I), followed by the SP4 thymocytes (24%), and DN cells (21%). With a depletion rate of 14% per day, SP8 thymocytes have a significantly lower turnover than SP4 thymocytes (*t* test on slope of regression on difference between SP4 and SP8 numbers, $p < 0.05$).

In the spleen, the depletion rates are lower: $CD4^+$ and $CD8^+$ naive T cells have a daily depletion rate of 9 and 7%, respectively (NS: *t* test, $p > 0.05$). The SP4 thymocyte depletion rate differs

Table II. *Parameter values, residence, and division times*[a]

Parameter	Value (95% CI)[b]	Symbol	Residence Time[c] (Days)	Division Time[d] (Days)
Input rate thymic precursors ($\times 10^6$/day)	0.02 (0.02–0.03)	σ_N		
Proliferation rate DN, SP, RTE (/day)	0.23 (0.19–0.25)	p_N, p_S, and p_R		
Proliferation rate DP (/day)	4.50[e]	p_P		
Selection DP into SP4 (fraction)	0.06 (0.03–0.08)	α_4		
Selection DP into SP8 (fraction)	0.01 (0.01–0.02)	α_8		
Fraction exported SP4 going to spleen	0.36 (0.29–0.41)	f_4		
Fraction exported SP8 going to spleen	0.74 (0.48–1.15)	f_8		
Differentiation parameter DN[f]	0.29 (0.25–0.33)	$\alpha_{\mu N}$		
Differentiation parameter DP[f]	0.20 (0.20–0.20)	$\alpha_{\mu P}$		
Differentiation parameter SP[f]	0.99 (0.98–1.00)	α_e		
Differentiation parameter RTE[f]	0.48 (0.35–0.49)	α_r		
Exponent of differentiation function	127 (61–200)	n		
Death rates of DN, early DP, SP, and RTE (/day)	0.00	δ[g]		
"Removal" rate last stage DP (LP)	0.37 (0.34–0.41)	μ_{LP}		
DN			17.6	4.4
Early DP			1.2	0.2
Last stage DP			2.7	Resting
SP			5.8	4.4
RTE			8.6	4.4

[a] Obtained by fitting scenario 5; see supplemental material, section 5.
[b] The 95% confidence intervals obtained with 500 bootstraps.
[c] Residence time: average time that a cell spends in a compartment; see supplemental material, section 6.
[d] Division time: average time between cellular divisions.
[e] No confidence interval, p_P always reaches the set maximum value.
[f] The differentiation rate ($\mu_N(i) = (\alpha_{\mu N}\, i)^n$, $\mu_P(i) = (\alpha_{\mu P}\, i)^n$ etc., see supplemental material, section 4) was arbitrarily set to 100/day as soon as it exceeded 100. This simplification did not influence the results: when the limit was set to 1000, the same results were found (results not shown). A differentiation rate above 100/day means the cells almost instantaneously differentiate. Therefore, the number of cells remaining in the DN subpopulation after the fourth division is virtually nil ($\mu_N(4) = (0.29 \times 4)^{127} = 1.5 \times 10^8$, so $\mu_N(4)$ set to 100).
[g] $\delta = \delta_N = \delta_P = \delta_S = \delta_R$.

significantly from the naive $CD4^+$ depletion rate (*t* test, $p < 0.05$), which was not the case for SP8 and naive $CD8^+$ splenocytes. Of note, GCV treatment results in a significant depletion of the $CD8^+CD44^{high}$ cells in the spleen (5% per day, $p < 0.05$, Table I), but not of $CD4^+CD44^{high}$ cells (2% per day, $p > 0.05$, Table I). These results suggest that the depletions observed in the naive and Ag-experienced T cell populations are unrelated.

Nadir and recovery

For the most immature DN and DP thymocytes, the nadir occurs at days 7 and 8, which corresponds to the end of the GCV treatment, and occurs later for mature T cells in the thymus and for naive splenocytes (14 days or later, Table I and Fig. 2*B*). Actually, the delay in cell recovery after GCV treatment becomes longer as the cell populations are more differentiated, in accordance with a DN→DP→SP→naive T splenocytes conveyor-belt type of thymocyte differentiation (30).

In contrast, for Ag-experienced T splenocytes the nadir was observed at day 7 (Table I): the compartment starts to refill just after the end of GCV treatment, confirming the difference between the dynamics of Ag-experienced and naive T cells.

After cessation of the 7-day GCV treatment, most thymocyte populations returned to levels similar to pretreatment values in ~4 wk (Fig. 2*B*, Mann-Whitney *U* test, $p > 0.05$ when comparing DN and SP cell numbers at days 0 and 28); only DP numbers were still slightly lower at day 28 than at day 0 ($p < 0.05$). In the spleen, $CD4^+$ and $CD8^+$ naive cells were still significantly depleted on day 28 ($p < 0.05$), but on day 70 their numbers had approached pretreatment values ($p > 0.05$). Thus, in young euthymic mice, thymocytes and spleen T lymphocytes can return to values close to steady state levels within 2 mo after short-term lymphopenia.

Estimation of the size of the long-lived naive cell population

Several observations led us to consider the $CD44^{low}CD45RB^{high}$ splenic T cells as a heterogeneous population, composed of a first subpopulation of rapidly proliferating RTE, differentiating into a second subpopulation of "long-lived", non- or slowly dividing naive cells, "resistant" to GCV and persisting after Tx (22).

The first observation is the match (Mann-Whitney *U* test, $p < 0.05$) between the sizes of the naive T cell populations in the spleen in euthymic mice after GCV therapy, and in Tx mice 4–5 wk after Tx (Fig. 2*B*, at 28 days after GCV, $CD4^+CD44^{low}$: 14.8 ± 4.6 million cells and $CD8^+CD44^{low}$: 4.6 ± 1.3 million cells; compare with Fig. 3*A*, Tx mice, day 0, 14.2 ± 1.7 million $CD4^+CD44^{low}$ cells and 4.8 ± 0.7 million $CD8^+CD44^{low}$ cells). These numbers represented ~50% of those observed in euthymic mice (Fig. 2*B*: day 0, 29 ± 3.1 millions $CD4^+CD44^{low}$ and 8.9 ± 0.6 millions $CD8^+CD44^{low}$). The second observation is that the number of naive $CD44^{low}$ T cells in Tx mice remained stable over the course of 14-day GCV treatment (ANOVA least significant difference method Fisher, $p > 0.05$ comparing day 0, 14, or 70 cell numbers; Fig. 3*A*), in contrast with euthymic mice (Mann-Whitney *U* test $p < 0.01$ comparing days 14 and 70; Fig. 3*A*). This suggests the existence of a population of resting long-lived naive cells, persisting after Tx and "resistant" to GCV.

The third observation is that the mice have approximately three and eight times more naive CD4 and CD8 T cells, respectively, in the spleen, than SP4 and SP8 cells in the thymus (Table I), and that half of them are strongly affected by GCV treatment, which is not compatible with the idea that nondividing RTE slowly accumulate from a small thymic source.

Altogether, our results indicate that RTE, which are depleted following Tx as well as GCV treatment, form a population of cells with a high turnover representing roughly 50% of the naive T cell population in young mice.

Table III. *Number of cells at steady state and differentiating, at each division stage*

Cell Compartment	Division Stage	Number of Cells (Millions)[a]	Number of Cells Differentiating to Next Compartment (Millions/Day)
Thymus			
DN	N_0	0.09	0.00
	N_1	0.18	0.00
	N_2	0.36	0.00
	N_3	0.72	0.00
	N_4	3×10^{-3}	0.32
Total DN		1.34	
Early DP	P_0	0.07	0.00[b]
	P_1	0.14	0.00[b]
	P_2	0.29	0.00[b]
	P_3	0.58	0.00[b]
	P_4	1.16	0.00[b]
	P_5	0.94	6.18[b]
	P_6	0.08	8.14[b]
Last stage DP	P_7[c]	40.29	15.05[d]
Total DP		43.57	
SP4	$S4_0$	4.02	0.00
	$S4_1$	2.49	1.26
	$S4_2$	0.01	1.13
Total SP4		6.53	
S8	$S8_0$	0.77	0.00
	$S8_1$	0.48	0.24
	$S8_2$	2×10^{-3}	0.22
Total SP8		1.25	
Total thymocytes		52.69	
Naive Spleen RTEs			
CD4 RTE	$R4_0$	3.79	0.00[e]
	$R4_1$	7.27	0.07[e]
	$R4_2$	0.03	3.30[e]
Total CD4 RTE		11.09	
Long-lived naive CD4		14.50	
Total CD4 $CD44^{low}$		25.59	
CD8 RTE	$R8_0$	1.49	0.00[e]
	$R8_1$	2.86	0.03[e]
	$R8_2$	0.01	1.30[e]
Total CD8 RTE		4.36	
Long-lived naive CD8		4.50	
Total CD8 $CD44^{low}$		8.86	

[a] From steady state expressions of model, obtained by fitting scenario 5. Only cell populations of more than 10^{-3} million cells are indicated.
[b] Cells in P_0 to P_6 stage that differentiate to last-stage DP.
[c] Strictly speaking not a "division stage," as last-stage DP do not divide.
[d] Cells undergoing selection: last stage DP cells that differentiate to SP stage or die.
[e] Differentiate into long-lived naive splenic cells, migrate to other organs, or die.

Best fit model and turnover parameters

Using the mathematical model described in *Materials and Methods*, we fitted five different scenarios to the data (comparative results given in supplemental material, section 7). We selected the scenario that gave the best fit (Fig. 4; scenario 5), that is 1) all cells—except last-stage DP cells—have negligible "natural" death rates on the time scale of the experiment; 2) RTE and thymocytes, except early DP cells, have similar proliferation rates.

We estimated residence and division times (Table II), cell numbers at each division stage, and differentiation rates in each population (Table III), cell turnover, production, and death rates (Table IV). The model and its main results are represented in Fig. 6. The best-fit model indicates that precursors enter the differentiation process as DN cells at a rate of 2×10^4/day (σ_N), i.e., 0.04% of all thymocytes (Table II). All DN divide four times (Fig. 5 and Table

Table IV. *Cell death and turnover parameters*

	Estimated Values[a]	Cell Turnover (/Day)	50% Replacement Time (Days)
Thymocytes dying[b] (/day)	14.0 million		
Thymocytes exported (/day)	2.9 million		
Thymocytes produced by division (/day)	16.8 million		
Cells produced by division before SP stage (/day)	15.0 million		
Percentage cells produced in thymus dying (/day)	83.1%		
Percentage cells produced before SP stage dying in the thymus (/day)	92.9%		
Splenic RTEs produced by division (/day)	3.5 million		
Thymocytes exported to spleen (/day)	1.2 million		
Contribution thymus vs division splenic RTE	25.5%		
Percentage thymocytes exported to periphery	5.4%		
Percentage positive selection last stage DP to SP (/day)			
SP4	2.3%		
SP8	0.4%		
DN		0.24	2.1
DP		0.35	1.4
SP4		0.37	1.3
SP8		0.37	1.3
CD4 RTE		0.30	1.7
CD8 RTE		0.30	1.7

[a] Results were obtained by fitting scenario 5; see supplemental material, section 5.
[b] All thymocyte death occurs at the transition between the last stage DP and the SP stage, as death rates are negligible at other stages.

III) during a period of ~18 days, with an average time between divisions ($1/p_N$, with proliferation rate $p_N = 0.23$/day) of ~4 days (Table II), before becoming DP. Early DP then actively proliferate during ~1 day; they divide on average every 5–6 h (proliferation rate $p_p = 4.5$/day, Table II), 59% of early DP completing five divisions and the rest six divisions (Fig. 5 and Table III), the maximum number of divisions we allowed in the model. After this period of intense proliferation, DP cells mature into nondividing DP cells (last-stage DP), a stage lasting on average 3 days (Table II).

Of the last-stage DP cells, 0.9×10^6 or 2.3% ($\mu_{LP}\alpha_4$) and 0.2×10^6 or 0.4% ($\mu_{LP}\alpha_8$) become SP4 and SP8 each day, respectively. This means that 35% ($\mu_{LP}(1\text{-}\alpha_4\text{-}\alpha_8)$) of last-stage DP cells die per day during selection (i.e., 14×10^6 DP cells, Fig. 6 and Table IV). Altogether, 93% of all cells produced before the SP stage die per day at the last DP stage, corresponding to 83% of all cells produced in the thymus (Table IV). Most SP cells then divide once (69%, Fig. 5) after on average 4 days (Table II).

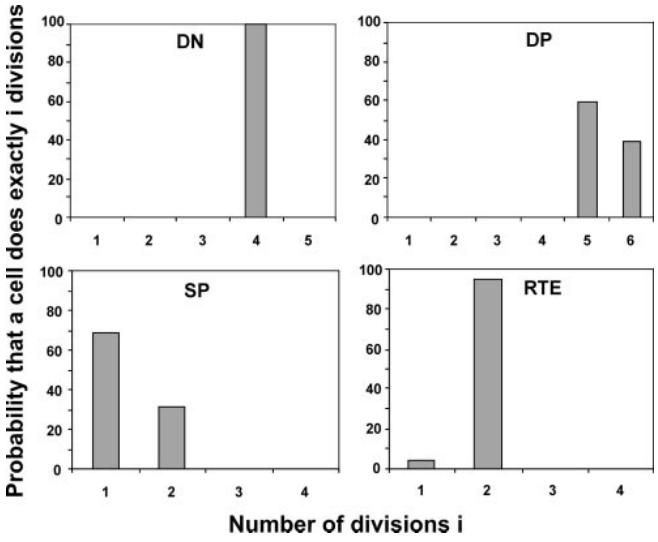

FIGURE 5. Number of divisions completed in the thymocyte subpopulations and in splenic RTE. We computed the probabilities that cells in each subpopulation (DN, DP, SP in thymus and RTE in spleen) complete exactly the number of divisions indicated. All DN divide four times, most DP five times, SP mostly once, and RTE mostly twice.

According to the model, 5% of thymocytes are exported to the periphery per day, which corresponds to a thymic output of 2.9×10^6 cells/day (roughly 145 times the input of 2×10^4/day; Fig. 6 and Table IV). We hypothesized that 42% of these RTE reach the spleen (11), where most undergo two divisions (96%, Fig. 5) over a period averaging 9 days, while keeping the naive $CD44^{low}$ $CD45RB^{high}$ phenotype (Table II and III). Then, they settle in the pool of long-lived naive cells, die, or migrate to another lymphoid compartment.

We estimated that 16.8×10^6 thymocytes are produced daily by intrathymic proliferation (Table IV). Besides, we estimated that 3.5×10^6 $CD44^{low}CD45RB^{high}$ T cells per day are produced by proliferation in the spleen, which is approximately three times more than the 1.2×10^6 cells/day contributed by the thymus to the spleen (42% of thymic export; Table IV).

SP and DP cells have the highest turnover with, respectively, 37 and 35% of cells being replaced per day, while DN cells have the lowest turnover (24% per day) (Table IV). Consequently, the time necessary to replace 50% of the population is similar between DP, SP, and RTE (around 1.5 days), and is slightly higher for DN (2.1 days).

Model validation: analysis of the percentages of cells in division

We determined the percentage of cells in division in the thymic and splenic subpopulations at steady state, by quantifying ex vivo the cell DNA contents. This is highest in DP (around 6% of all DP are in S plus G_2/M) and lowest ($\leq$1%) in SP4 and $CD44^{low}$ splenic T cells (Fig. 7, *A* and *B*).

To see whether our model estimates would match these results, we computed the percentage of cells entering division per day for each subpopulation, based on our fitting results (see formulas in supplemental material, section 5). We estimated that 34% of DP cells, 23% of DN, SP, and RTE cells enter division daily (Fig. 7*C*). If 43 and 49% of naive $CD4^+$ and $CD8^+$ T cells, respectively, consist of RTE (Table III), 9.9% ($0.43 \times 23\%$) of $CD4^+CD44^{low}$ cells and 11.3% ($0.49 \times 23\%$) of $CD8^+CD44^{low}$ cells would enter division daily (Fig. 7*C*). Thus, similar patterns were obtained with both methods.

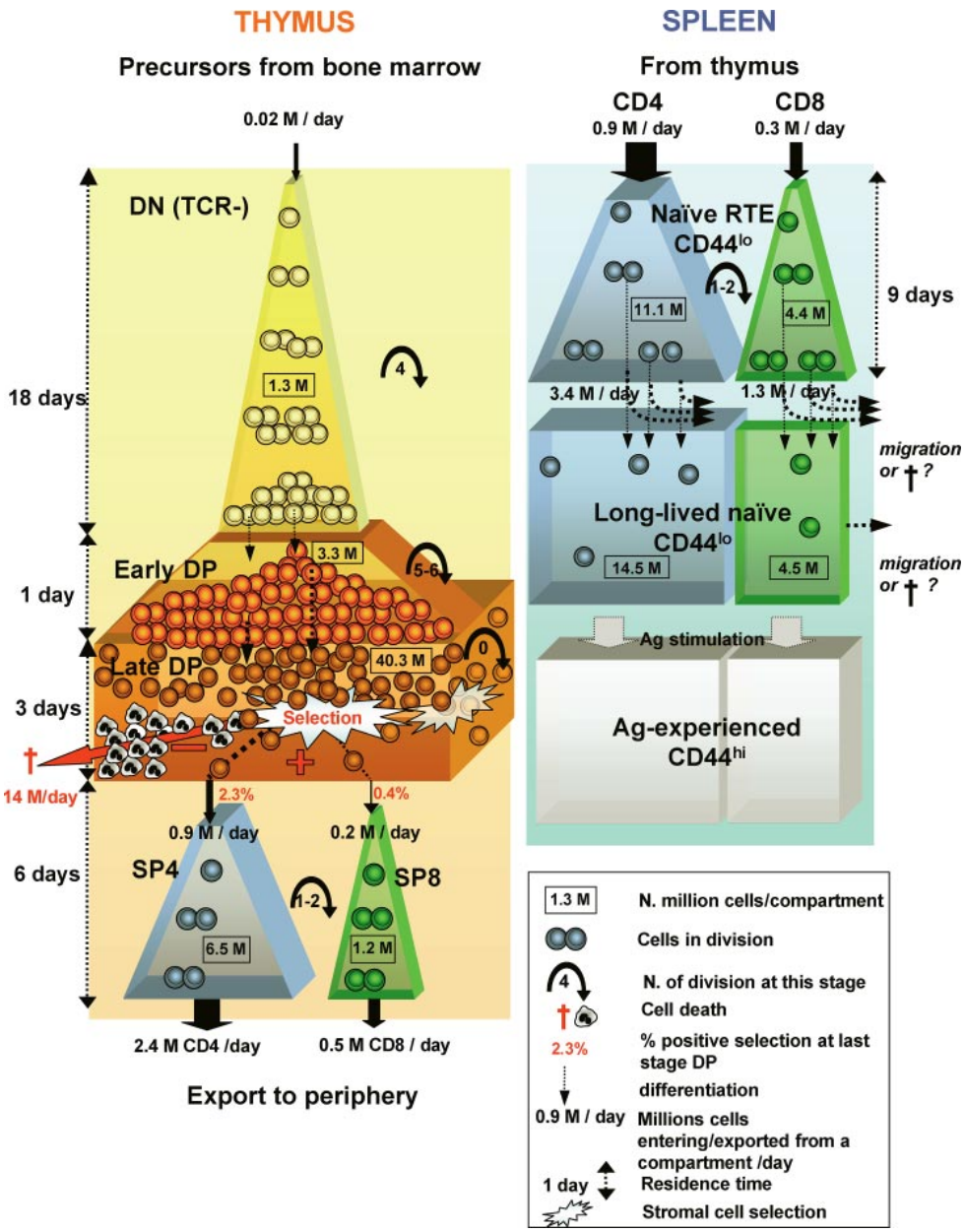

FIGURE 6. Representation of thymocyte and splenic naive T cell dynamics at steady state. Cell numbers, fluxes, and residence times obtained from the model fit to the data (Fig. 4; parameters, cell numbers and fluxes obtained from scenario 5, taken from Tables II–IV). Cell numbers in the boxes are steady state estimates based on our parameters (Table III). The Ag-experienced CD44^{high} cell population is indicated in gray because it was not studied in our mathematical model.

Model validation: simulated Tx

To validate our model results, we assessed whether they would reproduce the effect of Tx in mice (Fig. 3*B*): we simulated the naive T cell loss observed in the first 6 wk after Tx. The simulation predicts that the numbers of naive CD4$^+$ and CD8$^+$ T cells decrease in the spleen to, respectively, reach ~14.5 and 4.5 million 4–5 wk after Tx (Fig. 3*B*). These estimates are in accordance with the numbers of long-lived naive CD4$^+$ and CD8$^+$ T cells found in the spleen of mice 4–5 wk after Tx (14.2 and 4.8 million cells, respectively).

Discussion

Our experimental results demonstrate that the transient depletion of dividing thymocytes and T cells induces a fully reversible lymphopenia in young euthymic mice. Compared with other methods of T cell depletion, 1) the specific *TK* expression in the T cell compartment eliminates the potential side effects of chemo- or radioablation that affect other cell types; 2) the depletion is transient, controlled by the duration of GCV administration, in contrast with Tx; and 3) the depletion affects only dividing cells within the cell populations expressing *TK*. The animals regained almost normal numbers of thymocytes and mature T cells within ~1 and 2 mo after depletion, respectively, without alteration of the T cell repertoire (data not shown). This shows that the thymus of a young adult mouse, even after major depletion, remains fully functional and contributes to the production of RTE, as recently underlined in humans (35) and mice (26). The progressive delay in nadir of depletion observed in the thymocyte populations as they become more differentiated is consistent with a conveyor-belt model of division and differentiation of thymocytes: a cell enters the next, more mature, compartment after a time lag of differentiation and maturation that involves one or more division cycles. These observations are at the basis of our mathematical model. The present study reveals that traditional analysis of experimental results concerning the dynamics of complex lymphoid cell population can be improved markedly by mathematical modeling.

Considerations on the mathematical model

We formulated an 18-parameter mathematical model describing the dynamics of thymocytes and naive splenic T cells. Based on

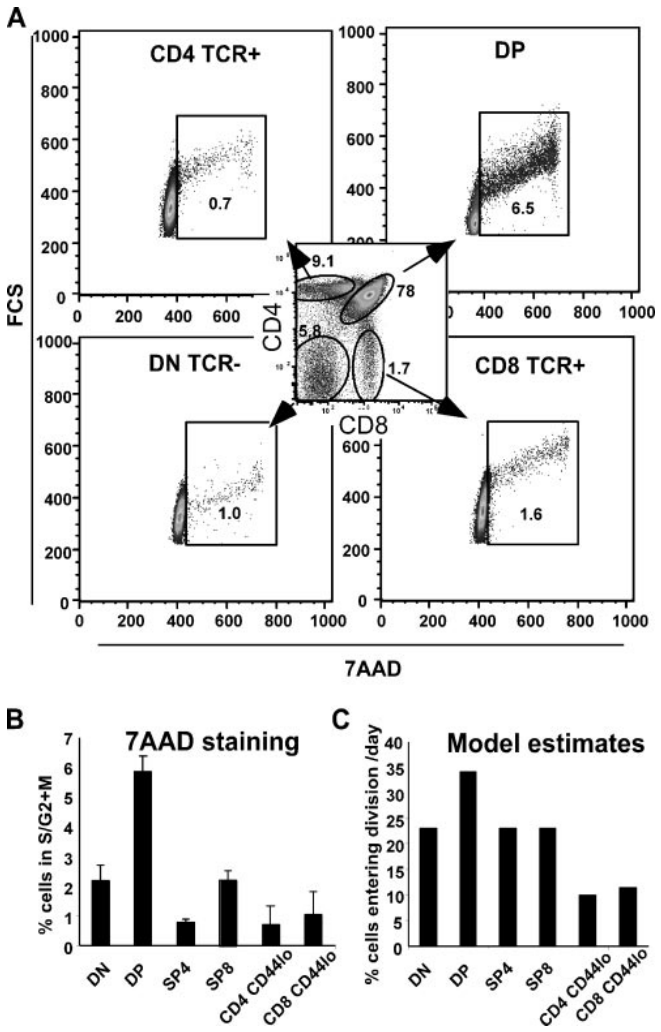

FIGURE 7. Cell division in thymocytes and naive splenocytes. *A* and *B*, Estimation of the percentage of cells in division ($S+G_2M$) in nontreated mice, by analysis of DNA content (7AAD labeling) by flow cytometry. *A*, Percentages of cells in $S+G_2M$ by gating on DN TCR^-, DP, SP TCR^+ cells (one of four experiments). *B*, Percentages of cells (mean of four to five experiments ± SEM) in $S+G_2M$ in thymocytes and $CD4^+CD44^{low}$ and $CD8^+CD44^{low}$ splenocytes (mean of two experiments ±SEM). *C*, Percentages of cells entering division per day, in DN TCR, DP, and SP thymocytes and in naive $CD44^{low}$ splenocytes, as estimated from the fit of scenario 5.

this model, we investigated the fit to our in vivo experimental data, of a number of scenarios with different sets of free parameters. We then selected the scenario which gave the best fit, using the lowest mean squares of residuals as a criterion. Although we could select a best-fit scenario, the fits were very similar in quality. Some scenarios gave quite divergent estimates for proliferation rates and residence times, especially for DP (supplemental material, section 8): residence times vary from 4 to 16 days, and proliferation rates from 0.3/day to 4.5/day. We therefore provide some additional support for the best-fit scenario. When $p_P = 4.5$/day, ~34% of DP cells enter division daily, and roughly 92% of DP cells are in the last, nondividing stage (last table supplementary material, scenarios 1, 2, and 5). When $p_P = 0.3$/day, the proportion DP entering division is halved (17%), while the percentage of cells in last stage DP is reduced to 40% (supplemental material, section 8, scenarios 3 and 4). Under GCV treatment, the observed daily rate of cell loss—which reflects the extent of division—is highest in the DP population (37% per day, Table I). Also, the majority (~85%) of DP are mature, nondividing cells (30). These two independent observations support the notion that early DP proliferate faster than other cell types, as assumed in scenarios 1, 2, and 5. Among these three scenarios yielding very similar parameter estimates, we took the best-fit scenario (scenario 5) to estimate the population dynamic parameters.

Earlier mathematical models describing thymocyte dynamics assumed that thymocytes proliferated in a density-dependent manner (36). It has since been shown that homeostatic regulation in the thymus only occurs when DN precursors are below 5% of their original counts (15). Similar observations were made in peripheral organs, where lymphopenia-induced proliferation only occurs when depletion exceeds 90% (26). The T cells in our *TK*-transgenic mice were not depleted to such an extent, so we did not allow for density-dependent homeostasis in our model.

Estimation of division rates and lifespans of thymic cell populations

The frequency of dividing cells estimated by DNA content and the model-based estimates of daily percentage of cells entering division show the same pattern (Fig. 7): DP have highest division rates, DN and SP have intermediate division rates, and naive cells in the spleen have the lowest.

Previously estimated times required for DN to differentiate into DP range from 5 to 6 days (37) to 15–16 days (17, 38). Our fitting procedure yielded an average residence time in the DN compartment of 18 days, with cells undergoing on average four divisions during that period. Previous reports showed that the total residence time in the DP compartment is 3 days (5), 3–4 days (30), or 3.5 days (6), and that cycling DP differentiate into SP in a minimum of 2 days (39). We found a residence time of 4 days for DP cells. We could split this period into two. According to our best-fit scenario, early DP undergo five to six divisions during their first day, in agreement with a previous report showing that all cycling DP disappeared 1 day after demecolcine treatment (37). In their second 3-day period, DP do not divide and are subject to selection. This would correspond to the period where cells have lower motility and prolonged contact with the thymic stroma, while positively-selected cells rapidly migrate from the cortex to the medulla (40).

Previous data showed a residence time of 6–7 days for the SP in the medulla (9). Our model indicates that positively selected SP cells undergo a postselection expansion (41, 42) during ~6 days before reaching the periphery, completing one to two divisions (whether TCR driven or not (8)), with an interdivision time averaging 4 days. Thus, an average of 27 days is required in these 3-mo-old adult mice to obtain a fully mature SP cell from a hematopoietic precursor cell.

Selection in the thymus and export rate to periphery

In our model, "natural" cell death in the thymus is only significant in the last, nondividing DP stage, likely reflecting the combined effect of death by neglect and negative selection. We estimated that 35% of the last stage nondividing DP die per day. To test the robustness of this finding, we looked at the scenario in which death may occur at every stage of thymocyte development and the proliferation rates differ across all cell populations (scenario 1, supplemental material, section 7). We still found that 97.5% of cells dying in the thymus do so at the last DP stage (the rest, 2.5%, dying at the SP stage; results not shown). Thus, our results are consistent with the notion that thymocyte selection occurs mainly at the DP stage (43, 44).

Given the diversity of experimental approaches and means of quantifying thymic selection, these estimates from the literature are difficult to interpret and compare with our findings. Positive

selection per se would concern 5% (45) to 20% of DP cells (10, 46), while estimates of subsequent negative selection are quite variable (10, 45, 47, 48). Our estimation that 83% of all thymocytes produced daily, or 93% of those produced before the SP stage (Table IV), die in the thymus, is in accordance with previous results (11) and the estimation that 90% of "developing thymocytes" (if taken as the daily production of thymocytes) die by neglect and 5% by negative selection (10). Our results reveal that after the combined process of positive and negative selection, only 2.5% of the last stage DP cells daily reach the early SP stage.

Our fitting procedure suggests that in 3-mo-old mice, ~3 million SP cells are exported from the thymus per day, i.e., 5.4% of the thymocytes. This is a rather high percentage compared with the previous estimates of 1% in 4.5-wk-old mice and 0.3% in 3.5-mo-old mice (11). In absolute cell numbers, previous estimates are also quite variable, ranging from 1 to 2–3 million per day (11, 12, 14) or even 5 million per day (22). These differences could stem from differences in age and strain of the mice used; also, lower estimates of cell export in the literature could be associated with stress induced by some experimental procedures.

Recently, it was shown that T cell differentiation continues postthymically with a preferential CD8 expansion (also observed in Fig. 7) and a lowered Bcl-2 expression in CD4, contributing to the decrease of the CD4:CD8 ratio at the periphery (13). We therefore investigated models of thymocyte and naive T cell dynamics, in which either the number of divisions, or the proliferation rates, differed between CD4 and CD8 cells in thymus and RTE in the spleen (data not shown). In the latter case, we imposed equal selection fractions ($\alpha_4 = \alpha_8$) and equal export fractions ($f_4 = f_8$). We still found the best fit for our original model, where the CD4:CD8 ratios in the thymus and spleen are set, respectively, by the difference in thymic selection coefficient (α_4 and α_8), and in fraction exported CD4 and CD8 thymocytes migrating to the spleen (f_4 and f_8). This means that five times more CD4 than CD8 thymocytes are generated from DP cells ($\alpha_4/\alpha_8 = 5$). This result is in accordance with earlier work (49), and with the recent hypothesis that CD4 or CD8 lineage commitment is determined by competition for MHC during epithelial cell interaction and cell dissociation rate, which is lower for CD8 than CD4 thymic T cells (50). Our data also suggest that twice as many CD8 as CD4 cells are exported to the spleen ($f_8/f_4 = 2$).

Splenic T cell turnover

Several lines of evidence suggested that the naive splenic T cell population in fact consists of dividing RTE and long-lived quiescent or slowly-dividing naive cells. Assuming that the naive T cell pool in Tx mice, or the cells remaining after GCV treatment, only consist of long-lived naive cells, we estimated that among naive T cells in the spleen ~43% of CD4 (11 million CD4 RTE) and 49% of CD8 (4 million CD8 RTE) are actively dividing RTE (Table III). Among all CD4 splenocytes, 31% are RTE and 41% long-lived naive cells, in accordance with percentages found in 3-mo-old mice (13). Our results suggest that splenic RTE divide twice, with an average interdivision time of 4 days, before settling in the long-lived naive cell pool, dying or migrating to other lymphoid organs. Our model results are compatible with the analysis of T cell depletion after hydroxyurea treatment, where Rocha et al. (22) estimated that 50% of peripheral T cells have a short survival time in vivo (48–72 h) and have recently divided.

Expansion of RTE and SP cells does not increase the repertoire diversity of naive T cells, as it is a postselection event; its main role could be to ensure a minimum size of the naive cell clone, for each cell having successfully passed the selection procedures, to guarantee Ag encounter and stimulation of an appropriate immune response.

We found an overall daily production of naive T cells of at least 6.4×10^6 cells/day (2.9×10^6 cells exported by the thymus and 3.5×10^6 cells produced by division of RTE in the spleen). This is a minimum estimate because the production of naive cells by division in other tissues or organs was not estimated. Our model results are compatible with a 25% contribution by the thymus to naive T cell production in the spleen.

The fast recovery of "Ag-experienced" splenic T cells just after cessation of GCV treatment, contrasting with the delayed recovery of upstream cell compartments, suggests their rapid homeostatic expansion and/or conversion from resting naive T cells in response to lymphopenia (51, 52), and possible recirculation between lymphoid organs and nonlymphoid tissues.

A systems biology approach to T cell differentiation and dynamics

Our work shows that understanding of a complex biological process, such as lymphocyte differentiation, can be fundamentally improved by mathematical modeling. Our model generates a comprehensive view of the T lymphocyte population quantifying the processes taking place during T cell differentiation. For example, it suggests that in young adult mice, 83% of thymocytes produced daily die at the transition from the DP to SP stage, making this the prime site of thymic selection. It also highlights the previously unrecognized major contribution of RTE expansion to the establishment of the peripheral naive T cell pool. We believe that our model, together with other systems biology approaches (50), can serve as a basis to further study T cell population dynamics, not only in physiological, but also in pathological settings.

Acknowledgments

We thank C. Durieu for technical help, M. C. Burland for quantitative RT-PCR, and B. Gouritin for cell sorting; personnel from the Nouvelle Animalerie Commune, Centre d'Exploration Fonctionnelle Pitié-Salpêtrière for breeding mice; R. Geskus for valuable statistical advice; and our colleagues for discussions.

Disclosures

The authors have no financial conflict of interest.

References

1. Freitas, A. A., and B. Rocha. 2000. Population biology of lymphocytes: the flight for survival. *Annu. Rev. Immunol.* 18: 83–111.
2. Goldrath, A. W., and M. J. Bevan. 1999. Selecting and maintaining a diverse T-cell repertoire. *Nature* 402: 255–262.
3. Sprent, J., and C. D. Surh. 2002. T cell memory. *Annu. Rev. Immunol.* 20: 551–579.
4. Egerton, M., and R. Scollay. 1990. Intrathymic selection of murine TCR $\alpha\beta^+$ $CD4^-CD8^-$ thymocytes. *Int. Immunol.* 2: 157–163.
5. Penit, C. 1990. Positive selection is an early event in thymocyte differentiation: high TCR expression by cycling immature thymocytes precedes final maturation by several days. *Int. Immunol.* 2: 629–638.
6. Huesmann, M., B. Scott, P. Kisielow, and H. von Boehmer. 1991. Kinetics and efficacy of positive selection in the thymus of normal and T cell receptor transgenic mice. *Cell* 66: 533–540.
7. Tough, D. F., and J. Sprent. 1994. Turnover of naive- and memory-phenotype T cells. *J. Exp. Med.* 179: 1127–1135.
8. Le Campion, A., B. Lucas, N. Dautigny, S. Leaument, F. Vasseur, and C. Penit. 2002. Quantitative and qualitative adjustment of thymic T cell production by clonal expansion of premigrant thymocytes. *J. Immunol.* 168: 1664–1671.
9. Rooke, R., C. Waltzinger, C. Benoist, and D. Mathis. 1997. Targeted complementation of MHC class II deficiency by intrathymic delivery of recombinant adenoviruses. *Immunity* 7: 123–134.
10. van Meerwijk, J. P., S. Marguerat, R. K. Lees, R. N. Germain, B. J. Fowlkes, and H. R. MacDonald. 1997. Quantitative impact of thymic clonal deletion on the T cell repertoire. *J. Exp. Med.* 185: 377–383.
11. Scollay, R., E. Butcher, and I. Weissman. 1980. Thymus cell migration: quantitative aspects of cellular traffic from the thymus to the periphery in mice. *Eur. J. Immunol.* 10: 210–218.

12. Graziano, M., Y. St-Pierre, C. Beauchemin, M. Desrosiers, and E. F. Potworowski. 1998. The fate of thymocytes labeled in vivo with CFSE. *Exp. Cell Res.* 240: 75–85.
13. Boursalian, T. E., J. Golob, D. M. Soper, C. J. Cooper, and P. J. Fink. 2004. Continued maturation of thymic emigrants in the periphery. *Nat. Immunol.* 5: 418–425.
14. Berzins, S. P., R. L. Boyd, and J. F. Miller. 1998. The role of the thymus and recent thymic migrants in the maintenance of the adult peripheral lymphocyte pool. *J. Exp. Med.* 187: 1839–1848.
15. Almeida, A. R., J. A. Borghans, and A. A. Freitas. 2001. T cell homeostasis: thymus regeneration and peripheral T cell restoration in mice with a reduced fraction of competent precursors. *J. Exp. Med.* 194: 591–599.
16. Freitas, A. A., and B. B. Rocha. 1993. Lymphocyte lifespans: homeostasis, selection and competition. *Immunol. Today* 14: 25–29.
17. Porritt, H. E., K. Gordon, and H. T. Petrie. 2003. Kinetics of steady-state differentiation and mapping of intrathymic-signaling environments by stem cell transplantation in nonirradiated mice. *J. Exp. Med.* 198: 957–962.
18. Hare, K. J., E. J. Jenkinson, and G. Anderson. 1999. In vitro models of T cell development. *Semin. Immunol.* 11: 3–12.
19. Jameson, S. C. 2005. T cell homeostasis: keeping useful T cells alive and live T cells useful. *Semin. Immunol.* 17: 231–237.
20. Min, B., and W. E. Paul. 2005. Endogenous proliferation: burst-like CD4 T cell proliferation in lymphopenic settings. *Semin. Immunol.* 17: 201–207.
21. Almeida, A. R., B. Rocha, A. A. Freitas, and C. Tanchot. 2005. Homeostasis of T cell numbers: from thymus production to peripheral compartmentalization and the indexation of regulatory T cells. *Semin. Immunol.* 17: 239–249.
22. Rocha, B., A. A. Freitas, and A. A. Coutinho. 1983. Population dynamics of T lymphocytes: renewal rate and expansion in the peripheral lymphoid organs. *J. Immunol.* 131: 2158–2164.
23. Heyman, R. A., E. Borrelli, J. Lesley, D. Anderson, D. D. Richman, S. M. Baird, R. Hyman, and R. M. Evans. 1989. Thymidine kinase obliteration: creation of transgenic mice with controlled immune deficiency. *Proc. Natl. Acad. Sci. USA* 86: 2698–2702.
24. Mackall, C. L., F. T. Hakim, and R. E. Gress. 1997. Restoration of T-cell homeostasis after T-cell depletion. *Semin. Immunol.* 9: 339–346.
25. Mehr, R., and A. S. Perelson. 1997. Blind T-cell homeostasis and the CD4/CD8 ratio in the thymus and peripheral blood. *J. Acquir. Immune Defic. Syndr. Hum. Retrovirol.* 14: 387–398.
26. Bourgeois, C., and B. Stockinger. 2006. $CD25^{+}CD4^{+}$ regulatory T cells and memory T cells prevent lymphopenia-induced proliferation of naive T cells in transient states of lymphopenia. *J. Immunol.* 177: 4558–4566.
27. Cohen, J. L., O. Boyer, B. Salomon, R. Onclercq, F. Charlotte, S. Bruel, G. Boisserie, and D. Klatzmann. 1997. Prevention of graft-versus-host disease in mice using a suicide gene expressed in T lymphocytes. *Blood* 89: 4636–4645.
28. Thomas-Vaslin, V., B. Bellier, J. L. Cohen, O. Boyer, N. Raynal-Raschilas, D. Glotz, and D. Klatzmann. 2000. Prolonged allograft survival through conditional and specific ablation of alloreactive T cells expressing a suicide gene. *Transplantation* 69: 2154–2161.
29. Bellier, B., V. Thomas-Vaslin, M. F. Saron, and D. Klatzmann. 2003. Turning immunological memory into amnesia by depletion of dividing T cells. *Proc. Natl. Acad. Sci. USA* 100: 15017–15022.
30. Scollay, R., and D. Godfrey. 1995. Thymic emigration: conveyor belts or lucky dips? *Immunol. Today* 16: 268–274.
31. Cohen, J. L., O. Boyer, B. Salomon, R. Onclenco, D. Depetris, L. Lejeune, V. Dubus-Bonnet, S. Bruel, F. Charlotte, M.-G. Matteî, and D. Klatzmann. 1998. Fertile homozygous transgenic mice expressing a functional truncated herpes simplex thymidine kinase ΔTK gene. *Transgenic Res.* 7: 321–330.
32. Salmon, P., O. Boyer, P. Lores, J. Jami, and D. Klatzmann. 1996. Characterization of an intronless CD4 minigene expressed in mature CD4 and CD8 T cells, but not expressed in immature thymocytes. *J. Immunol.* 156: 1873–1879.
33. Dominguez-Gerpe, L., and M. Rey-Mendez. 2001. Alterations induced by chronic stress in lymphocyte subsets of blood and primary and secondary immune organs of mice. *BMC Immunol.* 2: 7.
34. Balzarini, J., B. Degreve, G. Andrei, J. Neyts, M. Sandvold, F. Myhren, and E. de Clercq. 1998. Superior cytostatic activity of the ganciclovir elaidic acid ester due to the prolonged intracellular retention of ganciclovir anabolites in herpes simplex virus type 1 thymidine kinase gene-transfected tumor cells. *Gene Ther.* 5: 419–426.
35. Hakim, F. T., S. A. Memon, R. Cepeda, E. C. Jones, C. K. Chow, C. Kasten-Sportes, J. Odom, B. A. Vance, B. L. Christensen, C. L. Mackall, and R. E. Gress. 2005. Age-dependent incidence, time course, and consequences of thymic renewal in adults. *J. Clin. Invest.* 115: 930–939.
36. Mehr, R., A. S. Perelson, M. Fridkis-Hareli, and A. Globerson. 1997. Regulatory feedback pathways in the thymus. *Immunol. Today* 18: 581–585.
37. Vasseur, F., A. Le Campion, and C. Penit. 2001. Scheduled kinetics of cell proliferation and phenotypic changes during immature thymocyte generation. *Eur. J. Immunol.* 31: 3038–3047.
38. Shortman, K., M. Egerton, G. J. Spangrude, and R. Scollay. 1990. The generation and fate of thymocytes. *Semin. Immunol.* 2: 3–12.
39. Sprent, J., and D. F. Tough. 1994. Lymphocyte life-span and memory. *Science* 265: 1395–1400.
40. Witt, C. M., S. Raychaudhuri, B. Schaefer, A. K. Chakraborty, and E. A. Robey. 2005. Directed migration of positively selected thymocytes visualized in real time. *PLoS Biol.* 3: e160.
41. Penit, C., and F. Vasseur. 1997. Expansion of mature thymocyte subsets before emigration to the periphery. *J. Immunol.* 159: 4848–4856.
42. Hare, K. J., R. W. Wilkinson, E. J. Jenkinson, and G. Anderson. 1998. Identification of a developmentally regulated phase of postselection expansion driven by thymic epithelium. *J. Immunol.* 160: 3666–3672.
43. Kappler, J. W., N. Roehm, and P. Marrack. 1987. T cell tolerance by clonal elimination in the thymus. *Cell* 49: 273–280.
44. von Boehmer, H. 1994. Positive selection of lymphocytes. *Cell* 76: 219–228.
45. Laufer, T. M., J. DeKoning, J. S. Markowitz, D. Lo, and L. H. Glimcher. 1996. Unopposed positive selection and autoreactivity in mice expressing class II MHC only on thymic cortex. *Nature* 383: 81–85.
46. Merkenschlager, M., D. Graf, M. Lovatt, U. Bommhardt, R. Zamoyska, and A. G. Fisher. 1997. How many thymocytes audition for selection? *J. Exp. Med.* 186: 1149–1158.
47. Surh, C. D., and J. Sprent. 1994. T-cell apoptosis detected in situ during positive and negative selection in the thymus. *Nature* 372: 100–103.
48. Zhan, Y., J. F. Purton, D. I. Godfrey, T. J. Cole, W. R. Heath, and A. M. Lew. 2003. Without peripheral interference, thymic deletion is mediated in a cohort of double-positive cells without classical activation. *Proc. Natl. Acad. Sci. USA* 100: 1197–1202.
49. van Meerwijk, J. P., T. Bianchi, S. Marguerat, and H. R. MacDonald. 1998. Thymic lineage commitment rather than selection causes genetic variations in size of CD4 and CD8 compartments. *J. Immunol.* 160: 3649–3654.
50. Efroni, S., D. Harel, and I. R. Cohen. 2007. Emergent dynamics of thymocyte development and lineage determination. *PLoS Comput. Biol.* 3: e13.
51. Tanchot, C., A. Le Campion, S. Leaument, N. Dautigny, and B. Lucas. 2001. Naive $CD4^{+}$ lymphocytes convert to anergic or memory-like cells in T cell-deprived recipients. *Eur. J. Immunol.* 31: 2256–2265.
52. Bourgeois, C., and B. Stockinger. 2006. T cell homeostasis in steady state and lymphopenic conditions. *Immunol. Lett.* 107: 89–92.
53. Ernst, B., C. D. Surh, and J. Sprent. 1995. Thymic selection and cell division. *J. Exp. Med.* 182: 961–971.
54. Rocha, B., C. Penit, C. Baron, F. Vasseur, N. Dautigny, and A. F. Freitas. 1990. Accumulation of bromodeoxyuridine-labeled cells in central and peripheral lymphoid organs: minimal estimates of production and turnover rates of mature lymphocytes. *Eur. J. Immunol.* 20: 1697–1708.
55. Neese, R. A., L. M. Misell, S. Turner, A. Chu, J. Kim, D. Cesar, R. Hoh, F. Antelo, A. Strawford, J. M. McCune, et al. 2002. Measurement in vivo of proliferation rates of slow turnover cells by $2H_2O$ labeling of the deoxyribose moiety of DNA. *Proc. Natl. Acad. Sci. USA* 99: 15345–15350.
56. Armitage, P., and G. Berry. 1994. *Statistical Methods in Medical Research.* Blackwell, Oxford.

Supplemental material: Mathematical model and formulas

1. Parameters and variables

	Description	Dimension	Upper limit to parameter
Variable			
N_i	Number DN cells in division stage i[a]	Million cells	
P_i	Number DP cells in division stage i	Million cells	
$S4_i$	Number SP CD4 cells in division stage i	Million cells	
$S8_i$	Number SP CD8 cells in division stage i	Million cells	
$R4_i$	Number CD4 RTE in division stage i	Million cells	
$R8_i$	Number CD8 RTE in division stage i	Million cells	
Parameter			
$\sigma_N(t)$	Input of thymic precursor cells	Million cells / day	
p_i [b]	Proliferation rate of cell type i	Per day	p_P: 4.5[c]
δ_i	Death rate of cell type i	Per day	
$\mu_N(i)$[d]	Differentiation rate DN cells after division i	Per day	100
$\mu_P(i)$[e]	Differentiation rate DP cells after division i	Per day	100
μ_{LP}	Rate of loss of last stage DP cells	Per day	
$\alpha_{\mu N}$	Differentiation parameter DN		
$\alpha_{\mu P}$	Differentiation parameter DP		
n	Exponent of the differentiation functions		200
α_4	Fraction of differentiating DP that become SP4 (selection)	-	1
α_8	Fraction of differentiating DP that become SP8 (selection)	-	1
$e(i)$[f]	Export rate to periphery of SP cells after divison i	Per day	100
α_e	Differentiation parameter SP		
$f4$	Fraction of SP4 cells exported going to the spleen	-	1
$f8$	Fraction of SP8 cells exported going to the spleen	-	1
$r(i)$[g]	Rate of differentiation RTEs to long-lived naïve / death / migration		
α_r	Differentiation parameter RTE		

[a] Because immunostaining showed that about 60% of the DN cells have the expected TCR$^-$ phenotype (compare DN TCR- from Table 1 with DN numbers at day 0 in Figure 2B), we assumed in our model that 60% of the total DN population described in Figure 2B really contributes to the generation of DP thymocytes.

[b] We chose to have the same parameters of proliferation and "natural" death for the SP4 and SP8 cells (same proliferation rate p_S, number of divisions n_S and death rate δ_S for SP cells), and similarly for naïve CD4 and CD8 T cells in the spleen (same proliferation rate p_R, number of divisions n_R and death rate δ_R for RTEs). However, the literature is unclear as to whether rates of proliferation are the same between CD4 and CD8 thymocytes or between CD4 and CD8 naïve splenic T cells. In the thymus, a similar proliferation rate was found in mice (4, 54), in humans (55) while others found higher proliferation rates CD8 (8, 35, 41, 53). In spleen the proliferation was roughly equivalent (56) or a little higher in CD8 (13). We do test a scenario in which proliferation rates are different between CD4 and CD8 cells, see discussion.

[c] We set a maximum to the proliferation rate of DP cells of 4.5/day, which corresponds to an interdivision time of 5 to 6 hours.

[d] Determined by parameters $\alpha_{\mu N}$ and n

[e] Determined by parameters $\alpha_{\mu P}$ and n

[f] Determined by parameters α_e and n

[g] Determined by parameters α_r and n

2. Mathematical model

Double negative thymocytes:

$$\begin{cases} \dfrac{dN_0}{dt} = \sigma_N - (p_N + \delta_N) N_0 \\ \text{for i} = 1, 2, ... \text{n}_\text{N} : \\ \quad \dfrac{dN_i}{dt} = 2\gamma\, p_N N_{i-1} - (p_N + \delta_N + \mu_N(i)) N_i \end{cases}$$

Double positive thymocytes:

$$\begin{cases} \dfrac{dP_0}{dt} = \sum \mu N + 2\gamma\, p_N N_{n_N} - (p_P + \delta_P) P_0 \\ \text{for i} = 1, 2, ... \text{n}_P - 1 : \\ \quad \dfrac{dP_i}{dt} = 2\gamma\, p_P P_{i-1} - (p_P + \delta_P + \mu_P(i)) P_i \\ \dfrac{dP_{n_P}}{dt} = \sum \mu P + 2\gamma\, p_P P_{n_P - 1} - \mu_{LP} P_{n_P} \end{cases}$$

Under GCV, γ=0; when treatment stops, γ=1.

Single positive CD4 thymocytes:

$$\begin{cases} \dfrac{dS4_0}{dt} = \alpha_4 \mu_{LP} P_{n_P} - (p_S + \delta_S) S4_0 \\ \text{for i} = 1, 2, ... \text{n}_\text{S} - 1 : \\ \quad \dfrac{dS4_i}{dt} = 2\gamma\, p_S S4_{i-1} - (p_S + \delta_S + e(i)) S4_i \\ \dfrac{dS4_{n_S}}{dt} = 2\gamma\, p_S S4_{n_S - 1} - (\delta_S + e(n_S)) S4_{n_S} \end{cases}$$

CD4 RTE in spleen:

$$\begin{cases} \dfrac{dR4_0}{dt} = f_4 \sum eS4 - (p_R + \delta_R + r(1)) R4_0 \\ \text{for i} = 1, 2, ... \text{n}_\text{R} - 1 : \\ \quad \dfrac{dR4_i}{dt} = 2\gamma\, p_R R4_{i-1} - (p_R + \delta_R + r(i+1)) R4_i \\ \dfrac{dR4_{n_R}}{dt} = 2\gamma\, p_R R4_{n_R - 1} - (\delta_R + r(n_R + 1)) R4_{n_R} \end{cases}$$

with

$\mu_N(i) = (\alpha_{\mu N}\, i)^n$

and $\sum \mu N = \sum_{i=1}^{n_N} \mu_N(i) N_i$;

$\mu_P(i) = (\alpha_{\mu P}\, i)^n$

and $\sum \mu P = \sum_{i=1}^{n_P - 1} \mu_P(i) P_i$;

Single positive CD8 thymocytes:

$$\begin{cases} \dfrac{dS8_0}{dt} = \alpha_8 \mu_{LP} P_{n_P} - (p_S + \delta_S) S8_0 \\ \text{for i} = 1, 2, ... \text{n}_\text{S} - 1 : \\ \quad \dfrac{dS8_i}{dt} = 2\gamma\, p_S S8_{i-1} - (p_S + \delta_S + e(i)) S8_i \\ \dfrac{dS8_{n_S}}{dt} = 2\gamma\, p_S S8_{n_S - 1} - (\delta_S + e(n_S)) S8_{n_S} \end{cases}$$

CD8 RTE in spleen:

$$\begin{cases} \dfrac{dR8_0}{dt} = f_8 \sum eS8 - (p_R + \delta_R + r(1)) R8_0 \\ \text{for i} = 1, 2, ... \text{n}_\text{R} - 1 : \\ \quad \dfrac{dR8_i}{dt} = 2\gamma\, p_R R8_{i-1} - (p_R + \delta_R + r(i+1)) R8_i \\ \dfrac{dR8_{n_R}}{dt} = 2\gamma\, p_R R8_{n_R - 1} - (\delta_R + r(n_R + 1)) R8_{n_R} \end{cases}$$

with

$e(i) = (\alpha_e\, i)^n$

and $\sum eS4 = \sum_{i=1}^{n_S} e(i) S4_i$, $\sum eS8 = \sum_{i=1}^{n_S} e(i) S8_i$;

$r(i) = (\alpha_r\, i)^n$;

RTEs, as opposed to thymocytes, may already leave the RTE compartment in the 1st division stage.

3. Constraint on parameters: fraction of RTEs migrating to spleen

According to earlier work, 42% of RTEs go into the spleen upon exiting the thymus (11). This is a useful parameter to integrate into our model, as this will help us to determine the fraction of SP8 thymocytes exported homing to the spleen.

42% of RTEs going into the spleen translates into the following equation:

(thymocytes exported going to the spleen) / (overall thymus export) = 0.42

So $\frac{f_4 eS4_{n_S} + f_8 eS8_{n_S}}{eS4_{n_S} + eS8_{n_S}} = 0.42$

Yielding: $f_8 = \frac{0.42\left(S4_{n_S} + S8_{n_S}\right) - f_4 S4_{n_S}}{S8_{n_S}} = (0.42 - f_4)\frac{\alpha_4}{\alpha_8} + 0.42$

4. Number of divisions in relation to differentiation

As a cell divides, the rate of differentiation to the next compartment increases (rates are $\mu_N(i)$, $\mu_P(i)$, $e(i)$, $r(i)$ for the DN, DP, SP, and RTE respectively). Essentially, if i represents the division stage, $\mu_N(i)$, $\mu_P(i)$, $e(i)$, $r(i)$ are increasing functions of i: $\mu_N(i)=(\alpha_{\mu N}.i)^n$ for DN, $\mu_P(i)=(\alpha_{\mu P}.i)^n$ for DP, etc. where $\alpha_{\mu N}$, $\alpha_{\mu P}$ and n are fitted parameters. These parameters determine the number of divisions in each cell subpopulation.

As an example, we represent in the figure the values taken by the differentiation rate of cells at each division stage i in the DN and DP compartment, $\mu_N(i)$ and $\mu_P(i)$, respectively (for scenario 5, see definition of scenarios further down).

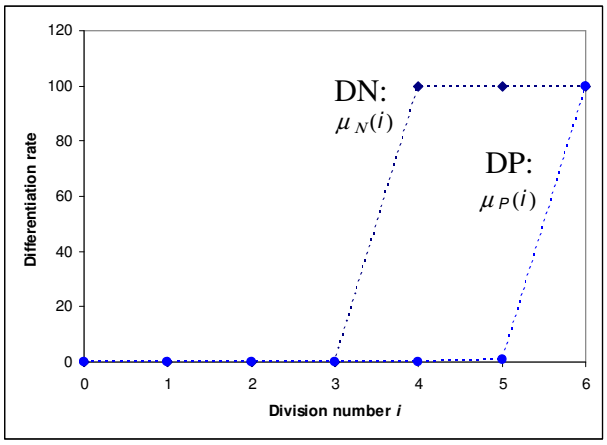

For the sake of simplication, and without significantly affecting the results, we set the value of the differentiation rate to 100/day whenever its actual value exceeded 100.

The "earlier" (for lower i) the differentiation rate jumps up –as is the case for DN compared to DP–, the fewer divisions occur. Overall, the fitted values yield very steep slopes for the differentiation functions, implying that all cells within a cellular compartment carry out a fixed number of divisions (a less steep function would imply more variation in the number of divisions a cell may complete within a cell compartment).

The probability that cells in each subpopulation complete a given number of divisions was derived as follows. Let p_{id} be the expected probability that a cell at stage i divides rather than differentiates or dies.

$p_{id} = \dfrac{p_i}{p_i + \delta_i + \mu(i)}$, where p_i is the probability of dividing, δ_i the probability of dying, and $\mu(i)$ the differentiation rate at stage i.

Say p_{iE} is the probability that a cell completes exactly i divisions.

Then $p_{iE} = p_{1d}\, p_{2d} \ldots\ p_{id}(1\text{-}p_{(i+1)d})$.

5. Mathematical formulas for terms in Table 2, Table 4, and Fig 7

Cell turnover (per day)

DN	$\sum_{i=0}^{n_N} \mu_N(i) N_i \,/\, totDN$
DP	$\delta_{LP} P_{n_P} \,/\, totDP$
SP	$\sum_{i=0}^{n_S} e(i) S4_i \,/\, totS4$
RTE	$\sum_{i=0}^{n_R} r(i+1) R4_i \,/\, totR4$

Division time = 1 / p_j
where *j* refers to the cell type DN, DP, SP, or RTE

Percentage cells entering division daily

DN	$100 \sum_{i=0}^{n_N} p_N N_i \,/\, totDN$
DP	$100 \sum_{i=0}^{n_P - 1} p_P P_i \,/\, totDP$
SP	$100 \sum_{i=0}^{n_S - 1} p_S S4_i \,/\, totS4$
RTE	$100 \sum_{i=0}^{n_R - 1} p_R R4_i \,/ (totR4 + 14.5)$

50% replacement time

	1 / (2*cell turnover)

Number late stage DP dying per day

$(1 - \alpha_4 - \alpha_8) \delta_{LP} P_{n_P}$

Number thymocytes produced by division per day

$p_N \sum_{i=0}^{n_N} N_i + p_P \sum_{i=0}^{n_P} P_i + p_S \sum_{i=0}^{n_S} (S4_i + S8_i)$

Number thymocytes produced by division per day before SP stage

$p_N \sum_{i=0}^{n_N} N_i + p_P \sum_{i=0}^{n_P} P_i$

Number RTE produced by division per day in spleen

$p_R \sum_{i=0}^{n_R} (R4_i + R8_i)$

Percentage positive selection on last stage DP

$(\alpha_4 + \alpha_8) \mu_{LP}$

Percentage thymocytes exported to periphery

$\sum_{i=0}^{n_S} e(i)(S4_i + S8_i)$ / total thymocytes

6. Computation of residence times of cells in different cellular compartments

We have to compute the total residence time, T, of cells in a general cascade where cells die at rate d and proceed to the next level at rate p, e.g.,

$$\frac{dx_0}{dt} = -(p+d)x_0,\ \frac{dx_i}{dt} = 2px_{i-1} - (p+d)x_i \text{ to } \frac{dx_n}{dt} = 2px_{n-1} - dx_n$$

for i=1,..., n-1. The contributions to the total residence time from the first and second compartment are

$$t_0 = \frac{1}{p+d} \text{ and } t_1 = \frac{p}{p+d}\frac{1}{p+d},$$

respectively. The non-dimensional $p/(p+d)=pt_0$ term in the second expression is the fraction of cells that proceed from the first to the second compartment. Similarly, the contribution of the third compartment is the fraction that proceed through the first and the second compartment times the time spent in this compartment, *i.e.*,

$$t_2 = pt_0\frac{p}{p+d}\frac{1}{p+d} = pt_1\frac{1}{p+d}$$

In general, we obtain that

$$t_i = pt_{i-1}\frac{1}{p+d} \text{ and } t_n = pt_{n-1}\frac{1}{d},$$

for i=1,…, n-1, and where the pt_i term is the fraction of cells arriving at that stage. The total residence time for this system $T=\sum_0^n t_i$ can indeed be simplified to the expected T=1/d.

For our more specific model where the maturation rates differ at each stage

$$\frac{dx_i}{dt} = 2px_{i-1} - (p+d+\mu_i)x_i$$

one would obtain

$$t_0 = \frac{1}{p+d+\mu_0},\ t_1 = \frac{p}{p+d+\mu_0}\frac{1}{p+d+\mu_1},\ t_2 = \frac{p}{p+d+\mu_0}\frac{p}{p+d+\mu_1}\frac{1}{p+d+\mu_2}$$

or the quite similar

$$t_i = pt_{i-1}\frac{1}{p+d+\mu_i}$$

where again the pt_{i-1} term remains the fraction of cells proceeding to the i^{th} compartment. Finally for the last stage of the double positive cells we have an equation of the form

$$\frac{dx_n}{dt} = \sum \mu_i x_i + 2px_{n-1} - \mu_n x_n \ ,$$

giving

$$t_n = \frac{1}{\mu_n}\left(pt_{n-1} + \frac{\mu_0}{p+d+\mu_0} + \sum_1^{i-1} \frac{pt_{i-1}\mu_i}{p+d+\mu_i} \right)$$

Thus, for the double negatives we obtain

$$t_0 = \frac{1}{p_N+\delta_N},\ t_i = \frac{pt_{i-1}}{p_N+\delta_N+\mu_N(i)} \text{ for } i=1,\ldots, n_N \quad \text{and where} \quad T_N = \sum_0^{n_N} t_i$$

For the double positives

$$t_0 = \frac{1}{p_P+\delta_P},\ t_i = \frac{pt_{i-1}}{p_P+\delta_P+\mu_P(i)} \text{ for } i=1,\ldots, n_P, \text{ and}$$

$$t_{n_P} = \frac{1}{\mu_{LP}}\left(pt_{n_P-1} + \sum_1^{n_P-1} \frac{pt_{i-1}\mu_i}{p_P+\delta_P+\mu_P(i)} \right)$$

and where $T_P = \sum_0^{n_P} t_i$.

For all but the last stages in the single positives and the RTE's, the same equations hold as for the DN. However, the last stages look different. This yields the following residence times:

SP:

$$t_0 = \frac{1}{p_S + \delta_S}, t_i = \frac{p_S t_{i-1}}{p_S + \delta_S + e(i)} \text{ with } i = 1,..., n_S - 1$$

$$t_{nS} = \frac{p_S t_{nS-1}}{\delta_S + e(n_S)}$$

$$T_S = \sum_0^{n_S} t_i$$

RTE:

$$t_0 = \frac{1}{p_R + \delta_R + r(1)}, t_i = \frac{p_R t_{i-1}}{p_R + \delta_R + r(i+1)} \text{ with } i = 1,..., n_R - 1$$

$$t_{nR} = \frac{p_R t_{nR-1}}{\delta_R + r(n_R + 1)}$$

$$T_R = \sum_0^{n_R} t_i$$

7. Definition and comparison of different scenarios

Scenario	Parameters conditions	Number parameters	Quality of fit	
			Sum of squares	Mean squares[a]
1. Full model	All parameters free	18	61.4	0.210
2. Negligible death rates	δ=0	14	61.4	0.208
3. One proliferation rate	$p=p_N=p_P=p_S=p_R$	15	68.8	0.233
4. Negligible death; one proliferation rate	δ=0 and $p=p_N=p_P=p_S=p_R$	11	67.9	0.227
5. DP differ in proliferation rate	$p_P \neq p$; δ=0; $p=p_N=p_S=p_R$	12	61.9	0.208

The model presented is rather complex, with 18 parameters (**Scenario 1**). An important assumption of this model is that the last stage DP cells do not divide and have a death rate different from the early stage DP. We fitted simplified versions of scenario 1:

In **scenario 2**, RTEs and thymocytes, except for the last stage non-dividing DP cells, have a negligible death rate on the time scale of the experiment (70 days), so $\delta_N=\delta_P=\delta_S=\delta_R=0$. All else is as in scenario 1, *i.e.* the model has 14 parameters.

In **scenario 3**, all cells have the same proliferation rate ($p=p_N=p_P=p_S=p_R$), all else being as in scenario 1, *i.e.* 15 parameters.

Scenario 4 is a combination of scenarios 2 and 3: cells have a negligible death rate and indistinguishable proliferation rates ($\delta_N=\delta_P=\delta_S=\delta_R=0$ and $p=p_N=p_P=p_S=p_R$).

In **scenario 5**, the proliferation rate of early DP cells, which are known to expand massively (and are most depleted by GCV treatment), is allowed to differ from that of other cells.

The quality of a fit is conventionally expressed as the "sum of squares" or "mean squares". The scenarios yielding the lowest sum of squares and mean squares are scenarios 2 (61.4

[a] The mean sum of squares is the sum of squares corrected for the number of free parameters: it is the residual sum of squares divided by the residual degrees of freedom, *i.e.* the difference between the number of data points and the number of free parameters (56).

and 0.208 respectively) and 5 (61.9 and 0.208 respectively). We chose the scenario with the lowest number of parameters, *i.e.* scenario 5.

Only scenario 4 has a lower number of parameters than scenario 5, but its fit yields a higher mean squares of residuals. We therefore assess whether the difference in sum of squares between scenarios 4 and 5 justifies the introduction of an additional parameter in scenario 5, namely proliferation rate of early DP cells. To that end, the sum of squares of the two scenarios were compared, using a partial F-test between these nested models (the F-value being the difference between the residual sum of squares per additional parameter, divided by the residual mean square of the largest of the two models (56). This shows that scenario 5 is the most plausible, because the p-value associated with this F-value is significant at α=0.01 ($F_{1, 298}$=28.9). So adding a single parameter –a different proliferation rate for early DP cells– does significantly improve the quality of the fit.

8. Proliferation and death rates, residence times and other parameters obtained by fitting different scenarios

Scenario	1	2	3	4	5 [a]
Proliferation (p) (/day)					
DN	0.21	0.21	0.28	0.30	0.23
DP early stages	4.50	4.50	0.28	0.30	4.50
SP	0.27	0.27	0.28	0.30	0.23
RTE	0.15	0.15	0.28	0.30	0.23
Death (δ) (/day)					
DN	2.8×10^{-7}	0.00	3.6×10^{-4}	0.00	0.00
DP early stages	8.6×10^{-7}	0.00	1.4×10^{-6}	0.00	0.00
SP	2.3×10^{-9}	0.00	1.6×10^{-4}	0.00	0.00
RTE	1.7×10^{-7}	0.00	5.8×10^{-8}	0.00	0.00
Residence time (days)					
DN	19.3	19.3	6.3	6.3	17.6
DP	4.0	4.0	16.2	15.6	3.9
SP	4.6	4.6	4.8	4.1	5.8
RTE	8.0	8.0	6.5	6.3	8.6
DP results					
Number early DP	3.1	3.2	25.9	22.4	3.3
Number last stage DP	39.5	39.6	15.5	17.6	40.3
Percentage DP in last stage	92.6	92.6	37.5	44.0	92.5
Proportion DP entering division /day	0.33	0.33	0.17	0.17	0.34
Other parameters					
σ_N	0.02	0.02	0.12	0.12	0.02
α_4	0.09	0.09	0.16	0.21	0.06
α_8	0.02	0.02	0.03	0.04	0.01
n	93.9	93.9	7.2	17.8	127.0
$\alpha_{\mu N}$	0.28	0.28	0.73	0.83	0.29
$\alpha_{\mu P}$	0.20	0.20	0.24	0.28	0.20
α_e	1.00	1.00	0.92	1.00	0.99
α_r	0.50	0.50	0.37	0.41	0.48
μ_{LP}	0.37	0.37	0.49	0.41	0.37
f_4	0.36	0.36	0.36	0.36	0.36
f_8	0.75	0.75	0.74	0.71	0.74

[a] Shaded scenario corresponds to the best overall fitting scenario

Supplemental material: Mathematical model and formulas

1. Parameters and variables

	Description	Dimension	Upper limit to parameter
Variable			
N_i	Number DN cells in division stage i[a]	Million cells	
P_i	Number DP cells in division stage i	Million cells	
$S4_i$	Number SP CD4 cells in division stage i	Million cells	
$S8_i$	Number SP CD8 cells in division stage i	Million cells	
$R4_i$	Number CD4 RTE in division stage i	Million cells	
$R8_i$	Number CD8 RTE in division stage i	Million cells	
Parameter			
$\sigma_N(t)$	Input of thymic precursor cells	Million cells / day	
p_i [b]	Proliferation rate of cell type i	Per day	p_P: 4.5[c]
δ_i	Death rate of cell type i	Per day	
$\mu_N(i)$[d]	Differentiation rate DN cells after division i	Per day	100
$\mu_P(i)$[e]	Differentiation rate DP cells after division i	Per day	100
μ_{LP}	Rate of loss of last stage DP cells	Per day	
$\alpha_{\mu N}$	Differentiation parameter DN		
$\alpha_{\mu P}$	Differentiation parameter DP		
n	Exponent of the differentiation functions		200
α_4	Fraction of differentiating DP that become SP4 (selection)	-	1
α_8	Fraction of differentiating DP that become SP8 (selection)	-	1
$e(i)$[f]	Export rate to periphery of SP cells after divison i	Per day	100
α_e	Differentiation parameter SP		
$f4$	Fraction of SP4 cells exported going to the spleen	-	1
$f8$	Fraction of SP8 cells exported going to the spleen	-	1
$r(i)$[g]	Rate of differentiation RTEs to long-lived naïve / death / migration		
α_r	Differentiation parameter RTE		

[a] Because immunostaining showed that about 60% of the DN cells have the expected TCR$^-$ phenotype (compare DN TCR- from Table 1 with DN numbers at day 0 in Figure 2B), we assumed in our model that 60% of the total DN population described in Figure 2B really contributes to the generation of DP thymocytes.

[b] We chose to have the same parameters of proliferation and "natural" death for the SP4 and SP8 cells (same proliferation rate p_S, number of divisions n_S and death rate δ_S for SP cells), and similarly for naïve CD4 and CD8 T cells in the spleen (same proliferation rate p_R, number of divisions n_R and death rate δ_R for RTEs). However, the literature is unclear as to whether rates of proliferation are the same between CD4 and CD8 thymocytes or between CD4 and CD8 naïve splenic T cells. In the thymus, a similar proliferation rate was found in mice (4, 54), in humans (55) while others found higher proliferation rates CD8 (8, 35, 41, 53). In spleen the proliferation was roughly equivalent (56) or a little higher in CD8 (13). We do test a scenario in which proliferation rates are different between CD4 and CD8 cells, see discussion.

[c] We set a maximum to the proliferation rate of DP cells of 4.5/day, which corresponds to an interdivision time of 5 to 6 hours.

[d] Determined by parameters $\alpha_{\mu N}$ and n

[e] Determined by parameters $\alpha_{\mu P}$ and n

[f] Determined by parameters α_e and n

[g] Determined by parameters α_r and n

2. Mathematical model

Double negative thymocytes:

$$\begin{cases} \dfrac{dN_0}{dt} = \sigma_N - (p_N + \delta_N) N_0 \\ \text{for i} = 1, 2, ... \text{n}_\text{N} : \\ \quad \dfrac{dN_i}{dt} = 2\gamma\, p_N N_{i-1} - (p_N + \delta_N + \mu_N(i)) N_i \end{cases}$$

Double positive thymocytes:

$$\begin{cases} \dfrac{dP_0}{dt} = \sum \mu N + 2\gamma\, p_N N_{n_N} - (p_P + \delta_P) P_0 \\ \text{for i} = 1, 2, ... \text{n}_P - 1 : \\ \quad \dfrac{dP_i}{dt} = 2\gamma\, p_P P_{i-1} - (p_P + \delta_P + \mu_P(i)) P_i \\ \dfrac{dP_{n_P}}{dt} = \sum \mu P + 2\gamma\, p_P P_{n_P - 1} - \mu_{LP} P_{n_P} \end{cases}$$

Under GCV, γ=0; when treatment stops, γ=1.

Single positive CD4 thymocytes:

$$\begin{cases} \dfrac{dS4_0}{dt} = \alpha_4 \mu_{LP} P_{n_P} - (p_S + \delta_S) S4_0 \\ \text{for i} = 1, 2, ... \text{n}_\text{S} - 1 : \\ \quad \dfrac{dS4_i}{dt} = 2\gamma\, p_S S4_{i-1} - (p_S + \delta_S + e(i)) S4_i \\ \dfrac{dS4_{n_S}}{dt} = 2\gamma\, p_S S4_{n_S - 1} - (\delta_S + e(n_S)) S4_{n_S} \end{cases}$$

CD4 RTE in spleen:

$$\begin{cases} \dfrac{dR4_0}{dt} = f_4 \sum eS4 - (p_R + \delta_R + r(1)) R4_0 \\ \text{for i} = 1, 2, ... \text{n}_\text{R} - 1 : \\ \quad \dfrac{dR4_i}{dt} = 2\gamma\, p_R R4_{i-1} - (p_R + \delta_R + r(i+1)) R4_i \\ \dfrac{dR4_{n_R}}{dt} = 2\gamma\, p_R R4_{n_R - 1} - (\delta_R + r(n_R + 1)) R4_{n_R} \end{cases}$$

with

$\mu_N(i) = (\alpha_{\mu N}\, i)^n$

and $\sum \mu N = \sum_{i=1}^{n_N} \mu_N(i) N_i$;

$\mu_P(i) = (\alpha_{\mu P}\, i)^n$

and $\sum \mu P = \sum_{i=1}^{n_P - 1} \mu_P(i) P_i$;

Single positive CD8 thymocytes:

$$\begin{cases} \dfrac{dS8_0}{dt} = \alpha_8 \mu_{LP} P_{n_P} - (p_S + \delta_S) S8_0 \\ \text{for i} = 1, 2, ... \text{n}_\text{S} - 1 : \\ \quad \dfrac{dS8_i}{dt} = 2\gamma\, p_S S8_{i-1} - (p_S + \delta_S + e(i)) S8_i \\ \dfrac{dS8_{n_S}}{dt} = 2\gamma\, p_S S8_{n_S - 1} - (\delta_S + e(n_S)) S8_{n_S} \end{cases}$$

CD8 RTE in spleen:

$$\begin{cases} \dfrac{dR8_0}{dt} = f_8 \sum eS8 - (p_R + \delta_R + r(1)) R8_0 \\ \text{for i} = 1, 2, ... \text{n}_\text{R} - 1 : \\ \quad \dfrac{dR8_i}{dt} = 2\gamma\, p_R R8_{i-1} - (p_R + \delta_R + r(i+1)) R8_i \\ \dfrac{dR8_{n_R}}{dt} = 2\gamma\, p_R R8_{n_R - 1} - (\delta_R + r(n_R + 1)) R8_{n_R} \end{cases}$$

with

$e(i) = (\alpha_e\, i)^n$

and $\sum eS4 = \sum_{i=1}^{n_S} e(i) S4_i$, $\sum eS8 = \sum_{i=1}^{n_S} e(i) S8_i$;

$r(i) = (\alpha_r\, i)^n$;

RTEs, as opposed to thymocytes, may already leave the RTE compartment in the 1st division stage.

3. Constraint on parameters: fraction of RTEs migrating to spleen

According to earlier work, 42% of RTEs go into the spleen upon exiting the thymus (11). This is a useful parameter to integrate into our model, as this will help us to determine the fraction of SP8 thymocytes exported homing to the spleen.

42% of RTEs going into the spleen translates into the following equation:

(thymocytes exported going to the spleen) / (overall thymus export) = 0.42

So $\frac{f_4 eS4_{n_S} + f_8 eS8_{n_S}}{eS4_{n_S} + eS8_{n_S}} = 0.42$

Yielding: $f_8 = \frac{0.42\left(S4_{n_S} + S8_{n_S}\right) - f_4 S4_{n_S}}{S8_{n_S}} = (0.42 - f_4)\frac{\alpha_4}{\alpha_8} + 0.42$

4. Number of divisions in relation to differentiation

As a cell divides, the rate of differentiation to the next compartment increases (rates are $\mu_N(i)$, $\mu_P(i)$, $e(i)$, $r(i)$ for the DN, DP, SP, and RTE respectively). Essentially, if i represents the division stage, $\mu_N(i)$, $\mu_P(i)$, $e(i)$, $r(i)$ are increasing functions of i: $\mu_N(i)=(\alpha_{\mu N}.i)^n$ for DN, $\mu_P(i)=(\alpha_{\mu P}.i)^n$ for DP, etc. where $\alpha_{\mu N}$, $\alpha_{\mu P}$ and n are fitted parameters. These parameters determine the number of divisions in each cell subpopulation.

As an example, we represent in the figure the values taken by the differentiation rate of cells at each division stage i in the DN and DP compartment, $\mu_N(i)$ and $\mu_P(i)$, respectively (for scenario 5, see definition of scenarios further down).

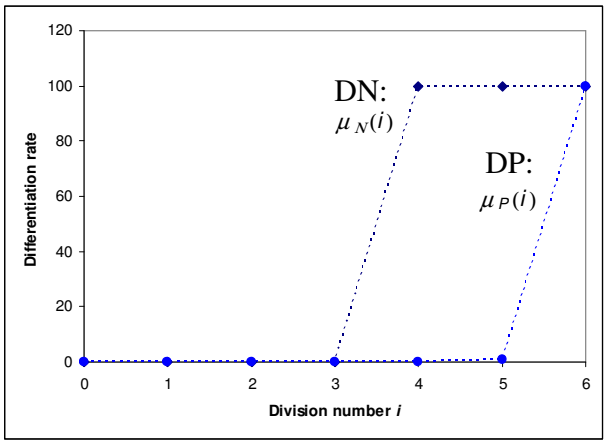

For the sake of simplication, and without significantly affecting the results, we set the value of the differentiation rate to 100/day whenever its actual value exceeded 100.

The "earlier" (for lower i) the differentiation rate jumps up –as is the case for DN compared to DP–, the fewer divisions occur. Overall, the fitted values yield very steep slopes for the differentiation functions, implying that all cells within a cellular compartment carry out a fixed number of divisions (a less steep function would imply more variation in the number of divisions a cell may complete within a cell compartment).

The probability that cells in each subpopulation complete a given number of divisions was derived as follows. Let p_{id} be the expected probability that a cell at stage i divides rather than differentiates or dies.

$p_{id} = \dfrac{p_i}{p_i + \delta_i + \mu(i)}$, where p_i is the probability of dividing, δ_i the probability of dying, and $\mu(i)$ the differentiation rate at stage i.

Say p_{iE} is the probability that a cell completes exactly i divisions.

Then $p_{iE} = p_{1d}\, p_{2d} \ldots\ p_{id}(1\text{-}p_{(i+1)d})$.

5. Mathematical formulas for terms in Table 2, Table 4, and Fig 7

Cell turnover (per day)

DN	$\sum_{i=0}^{n_N} \mu_N(i) N_i \,/\, totDN$
DP	$\delta_{LP} P_{n_P} \,/\, totDP$
SP	$\sum_{i=0}^{n_S} e(i) S4_i \,/\, totS4$
RTE	$\sum_{i=0}^{n_R} r(i+1) R4_i \,/\, totR4$

Division time = 1 / p_j
where *j* refers to the cell type DN, DP, SP, or RTE

Percentage cells entering division daily

DN	$100 \sum_{i=0}^{n_N} p_N N_i \,/\, totDN$
DP	$100 \sum_{i=0}^{n_P - 1} p_P P_i \,/\, totDP$
SP	$100 \sum_{i=0}^{n_S - 1} p_S S4_i \,/\, totS4$
RTE	$100 \sum_{i=0}^{n_R - 1} p_R R4_i \,/ (totR4 + 14.5)$

50% replacement time

	1 / (2*cell turnover)

Number late stage DP dying per day

$(1 - \alpha_4 - \alpha_8) \delta_{LP} P_{n_P}$

Number thymocytes produced by division per day

$p_N \sum_{i=0}^{n_N} N_i + p_P \sum_{i=0}^{n_P} P_i + p_S \sum_{i=0}^{n_S} (S4_i + S8_i)$

Number thymocytes produced by division per day before SP stage

$p_N \sum_{i=0}^{n_N} N_i + p_P \sum_{i=0}^{n_P} P_i$

Number RTE produced by division per day in spleen

$p_R \sum_{i=0}^{n_R} (R4_i + R8_i)$

Percentage positive selection on last stage DP

$(\alpha_4 + \alpha_8) \mu_{LP}$

Percentage thymocytes exported to periphery

$\sum_{i=0}^{n_S} e(i)(S4_i + S8_i)$ / total thymocytes

6. Computation of residence times of cells in different cellular compartments

We have to compute the total residence time, T, of cells in a general cascade where cells die at rate d and proceed to the next level at rate p, e.g.,

$$\frac{dx_0}{dt} = -(p+d)x_0,\ \frac{dx_i}{dt} = 2px_{i-1} - (p+d)x_i \text{ to } \frac{dx_n}{dt} = 2px_{n-1} - dx_n$$

for i=1,..., n-1. The contributions to the total residence time from the first and second compartment are

$$t_0 = \frac{1}{p+d} \text{ and } t_1 = \frac{p}{p+d}\frac{1}{p+d},$$

respectively. The non-dimensional $p/(p+d)=pt_0$ term in the second expression is the fraction of cells that proceed from the first to the second compartment. Similarly, the contribution of the third compartment is the fraction that proceed through the first and the second compartment times the time spent in this compartment, *i.e.*,

$$t_2 = pt_0\frac{p}{p+d}\frac{1}{p+d} = pt_1\frac{1}{p+d}$$

In general, we obtain that

$$t_i = pt_{i-1}\frac{1}{p+d} \text{ and } t_n = pt_{n-1}\frac{1}{d},$$

for i=1,…, n-1, and where the pt_i term is the fraction of cells arriving at that stage. The total residence time for this system $T=\sum_0^n t_i$ can indeed be simplified to the expected T=1/d.

For our more specific model where the maturation rates differ at each stage

$$\frac{dx_i}{dt} = 2px_{i-1} - (p+d+\mu_i)x_i$$

one would obtain

$$t_0 = \frac{1}{p+d+\mu_0},\ t_1 = \frac{p}{p+d+\mu_0}\frac{1}{p+d+\mu_1},\ t_2 = \frac{p}{p+d+\mu_0}\frac{p}{p+d+\mu_1}\frac{1}{p+d+\mu_2}$$

or the quite similar

$$t_i = pt_{i-1}\frac{1}{p+d+\mu_i}$$

where again the pt_{i-1} term remains the fraction of cells proceeding to the i^{th} compartment. Finally for the last stage of the double positive cells we have an equation of the form

$$\frac{dx_n}{dt} = \sum \mu_i x_i + 2px_{n-1} - \mu_n x_n \ ,$$

giving

$$t_n = \frac{1}{\mu_n}\left(pt_{n-1} + \frac{\mu_0}{p+d+\mu_0} + \sum_1^{i-1} \frac{pt_{i-1}\mu_i}{p+d+\mu_i} \right)$$

Thus, for the double negatives we obtain

$$t_0 = \frac{1}{p_N+\delta_N},\ t_i = \frac{pt_{i-1}}{p_N+\delta_N+\mu_N(i)} \text{ for } i=1,\ldots, n_N \quad \text{and where} \quad T_N = \sum_0^{n_N} t_i$$

For the double positives

$$t_0 = \frac{1}{p_P+\delta_P},\ t_i = \frac{pt_{i-1}}{p_P+\delta_P+\mu_P(i)} \text{ for } i=1,\ldots, n_P, \text{ and}$$

$$t_{n_P} = \frac{1}{\mu_{LP}}\left(pt_{n_P-1} + \sum_1^{n_P-1} \frac{pt_{i-1}\mu_i}{p_P+\delta_P+\mu_P(i)} \right)$$

and where $T_P = \sum_0^{n_P} t_i$.

For all but the last stages in the single positives and the RTE's, the same equations hold as for the DN. However, the last stages look different. This yields the following residence times:

SP:

$$t_0 = \frac{1}{p_S + \delta_S}, t_i = \frac{p_S t_{i-1}}{p_S + \delta_S + e(i)} \text{ with } i = 1,..., n_S - 1$$

$$t_{nS} = \frac{p_S t_{nS-1}}{\delta_S + e(n_S)}$$

$$T_S = \sum_0^{n_S} t_i$$

RTE:

$$t_0 = \frac{1}{p_R + \delta_R + r(1)}, t_i = \frac{p_R t_{i-1}}{p_R + \delta_R + r(i+1)} \text{ with } i = 1,..., n_R - 1$$

$$t_{nR} = \frac{p_R t_{nR-1}}{\delta_R + r(n_R + 1)}$$

$$T_R = \sum_0^{n_R} t_i$$

7. Definition and comparison of different scenarios

Scenario	Parameters conditions	Number parameters	Quality of fit	
			Sum of squares	Mean squares[a]
1. Full model	All parameters free	18	61.4	0.210
2. Negligible death rates	δ=0	14	61.4	0.208
3. One proliferation rate	$p=p_N=p_P=p_S=p_R$	15	68.8	0.233
4. Negligible death; one proliferation rate	δ=0 and $p=p_N=p_P=p_S=p_R$	11	67.9	0.227
5. DP differ in proliferation rate	$p_P \neq p$; δ=0; $p=p_N=p_S=p_R$	12	61.9	0.208

The model presented is rather complex, with 18 parameters (**Scenario 1**). An important assumption of this model is that the last stage DP cells do not divide and have a death rate different from the early stage DP. We fitted simplified versions of scenario 1:

In **scenario 2**, RTEs and thymocytes, except for the last stage non-dividing DP cells, have a negligible death rate on the time scale of the experiment (70 days), so $\delta_N=\delta_P=\delta_S=\delta_R=0$. All else is as in scenario 1, *i.e.* the model has 14 parameters.

In **scenario 3**, all cells have the same proliferation rate ($p=p_N=p_P=p_S=p_R$), all else being as in scenario 1, *i.e.* 15 parameters.

Scenario 4 is a combination of scenarios 2 and 3: cells have a negligible death rate and indistinguishable proliferation rates ($\delta_N=\delta_P=\delta_S=\delta_R=0$ and $p=p_N=p_P=p_S=p_R$).

In **scenario 5**, the proliferation rate of early DP cells, which are known to expand massively (and are most depleted by GCV treatment), is allowed to differ from that of other cells.

The quality of a fit is conventionally expressed as the "sum of squares" or "mean squares". The scenarios yielding the lowest sum of squares and mean squares are scenarios 2 (61.4

[a] The mean sum of squares is the sum of squares corrected for the number of free parameters: it is the residual sum of squares divided by the residual degrees of freedom, *i.e.* the difference between the number of data points and the number of free parameters (56).

and 0.208 respectively) and 5 (61.9 and 0.208 respectively). We chose the scenario with the lowest number of parameters, *i.e.* scenario 5.

Only scenario 4 has a lower number of parameters than scenario 5, but its fit yields a higher mean squares of residuals. We therefore assess whether the difference in sum of squares between scenarios 4 and 5 justifies the introduction of an additional parameter in scenario 5, namely proliferation rate of early DP cells. To that end, the sum of squares of the two scenarios were compared, using a partial F-test between these nested models (the F-value being the difference between the residual sum of squares per additional parameter, divided by the residual mean square of the largest of the two models (56). This shows that scenario 5 is the most plausible, because the p-value associated with this F-value is significant at α=0.01 ($F_{1, 298}$=28.9). So adding a single parameter –a different proliferation rate for early DP cells– does significantly improve the quality of the fit.

8. Proliferation and death rates, residence times and other parameters obtained by fitting different scenarios

Scenario	1	2	3	4	5 [a]
Proliferation (p) (/day)					
DN	0.21	0.21	0.28	0.30	0.23
DP early stages	4.50	4.50	0.28	0.30	4.50
SP	0.27	0.27	0.28	0.30	0.23
RTE	0.15	0.15	0.28	0.30	0.23
Death (δ) (/day)					
DN	2.8×10^{-7}	0.00	3.6×10^{-4}	0.00	0.00
DP early stages	8.6×10^{-7}	0.00	1.4×10^{-6}	0.00	0.00
SP	2.3×10^{-9}	0.00	1.6×10^{-4}	0.00	0.00
RTE	1.7×10^{-7}	0.00	5.8×10^{-8}	0.00	0.00
Residence time (days)					
DN	19.3	19.3	6.3	6.3	17.6
DP	4.0	4.0	16.2	15.6	3.9
SP	4.6	4.6	4.8	4.1	5.8
RTE	8.0	8.0	6.5	6.3	8.6
DP results					
Number early DP	3.1	3.2	25.9	22.4	3.3
Number last stage DP	39.5	39.6	15.5	17.6	40.3
Percentage DP in last stage	92.6	92.6	37.5	44.0	92.5
Proportion DP entering division /day	0.33	0.33	0.17	0.17	0.34
Other parameters					
σ_N	0.02	0.02	0.12	0.12	0.02
α_4	0.09	0.09	0.16	0.21	0.06
α_8	0.02	0.02	0.03	0.04	0.01
n	93.9	93.9	7.2	17.8	127.0
$\alpha_{\mu N}$	0.28	0.28	0.73	0.83	0.29
$\alpha_{\mu P}$	0.20	0.20	0.24	0.28	0.20
α_e	1.00	1.00	0.92	1.00	0.99
α_r	0.50	0.50	0.37	0.41	0.48
μ_{LP}	0.37	0.37	0.49	0.41	0.37
f_4	0.36	0.36	0.36	0.36	0.36
f_8	0.75	0.75	0.74	0.71	0.74

[a] Shaded scenario corresponds to the best overall fitting scenario